Mechanisms of amyloid fibril formation by proteins

Santosh Kumar and Jayant B. Udgaonkar*

National Centre for Biological Sciences, Tata Institute of Fundamental Research, Bangalore 560 065, India

Understanding the structural heterogeneity inherent in the process of amyloid fibril formation is an important goal of protein aggregation studies. Structural heterogeneity in amyloid fibrils formed by a protein manifests itself in fibrils varying in internal structure and external appearance, and may originate from molecular level variations in the internal structure of the cross-β motif. Amyloid fibril formation commences from partially structured conformations of a protein, and in many cases, proceeds via pre-fibrillar aggregates (spherical oligomers and/or protofibrils). It now appears that structural heterogeneity is prevalent in the partially structured conformations as well as in the pre-fibrillar aggregates of proteins. Amyloid fibril formation may therefore potentially commence from many precursor states, and amyloid fibril polymorphism might be the consequence of the utilization of distinct nucleation and elongation mechanisms. This review examines the current understanding of the structural heterogeneity seen in amyloid fibril formation reactions, and describes how an understanding of the initial and intermediate stages of amyloid fibril formation reactions can provide an insight into the structural heterogeneity seen in mature fibrils.

Keywords: Alternative pathways, amyloid fibrils, amyloid protofibrils, spherical oligomers, structural heterogeneity.

THE process of protein aggregation is a widely observed phenomenon in biology. A well-studied example is the aggregation of cytoskeletal proteins into filaments, which are vital for many cellular processes[1–3]. But protein aggregation is also seen in disruptive contexts, where it affects the folding or normal functioning of proteins. *In vitro* studies of the refolding or unfolding of proteins at high concentrations are often hindered by the transient accumulation of protein aggregates[4–7]. Protein aggregation is often a complication during the purification of recombinant proteins[8], and avoiding aggregation can be a challenge during the industrial production of therapeutic proteins. While many such protein aggregates are disordered, protein aggregates can also be highly ordered[9]. One example of ordered protein aggregates possessing a remarkably high internal order is the amyloid fibril.

Understanding the principles of amyloid fibril formation is an important problem in modern biology. Many human diseases, including Alzheimer's disease, Parkinson's disease, Huntington's disease as well as the prion diseases, are associated with the formation of amyloid fibrils[10]. In amyloidoses, amyloid fibrils accumulate in the brain, or in one or more other tissues[11]. Amyloid fibrils are, however, not always harmful. It is now increasingly being seen that living organisms, ranging from prokaryotes to humans, exploit amyloid fibrils formed by their endogenous proteins for carrying out normal physiological functions[11,12]. From the biotechnology perspective, amyloid fibrils also appear promising as macromolecular assembly based nanomaterials[13–15].

The term 'amyloid' was first used by Rudolf Virchow to describe a structured mass in human tissues, which was considered to be a cellulose-containing substance on the basis of its ability to be stained by iodine[16,17]. Later, direct chemical analysis showed that the main component of amyloids is protein[18,19]. Now, amyloid fibrils refer to elongated protein aggregates characterized by their long and relatively straight morphologies, cross-β diffraction patterns, specific dye binding properties and rigid core structures. They show a characteristic X-ray diffraction pattern[20,21] with 4.7–4.8 Å meridional reflections and 10 Å equatorial reflections. They bind to and alter the spectroscopic characteristics of congo-red[22,23] and thioflavin dyes[24,25]. Hydrogen exchange experiments coupled with mass spectrometry (HX-MS)[26] and with NMR (HX-NMR)[27,28] have suggested that amyloid fibrils possess extensively hydrogen-bonded β-sheet core structures, which confer to them remarkable stability and resistance to protease cleavage[29,30].

Amyloid fibril formation involves a structural rearrangement of the native state into a β-sheet rich fibrillar conformation[31]. β-sheets seem to provide a scaffold that is favourable for protein assembly: the edge strands of β-sheet structures are unstable, and the sheet can grow by interacting with any other β-strands it encounters[32]. Natural β-sheet proteins are seen to utilize a number of mechanisms to avoid the edge-to-edge aggregation of their β-sheets[33,34]. It now appears that all proteins can potentially assemble into amyloid fibrils[11,35].

Amyloid fibril formation is an extremely complex reaction. A protein can assemble into multiple structurally distinct fibrils[36,37]. Structural heterogeneity also appears
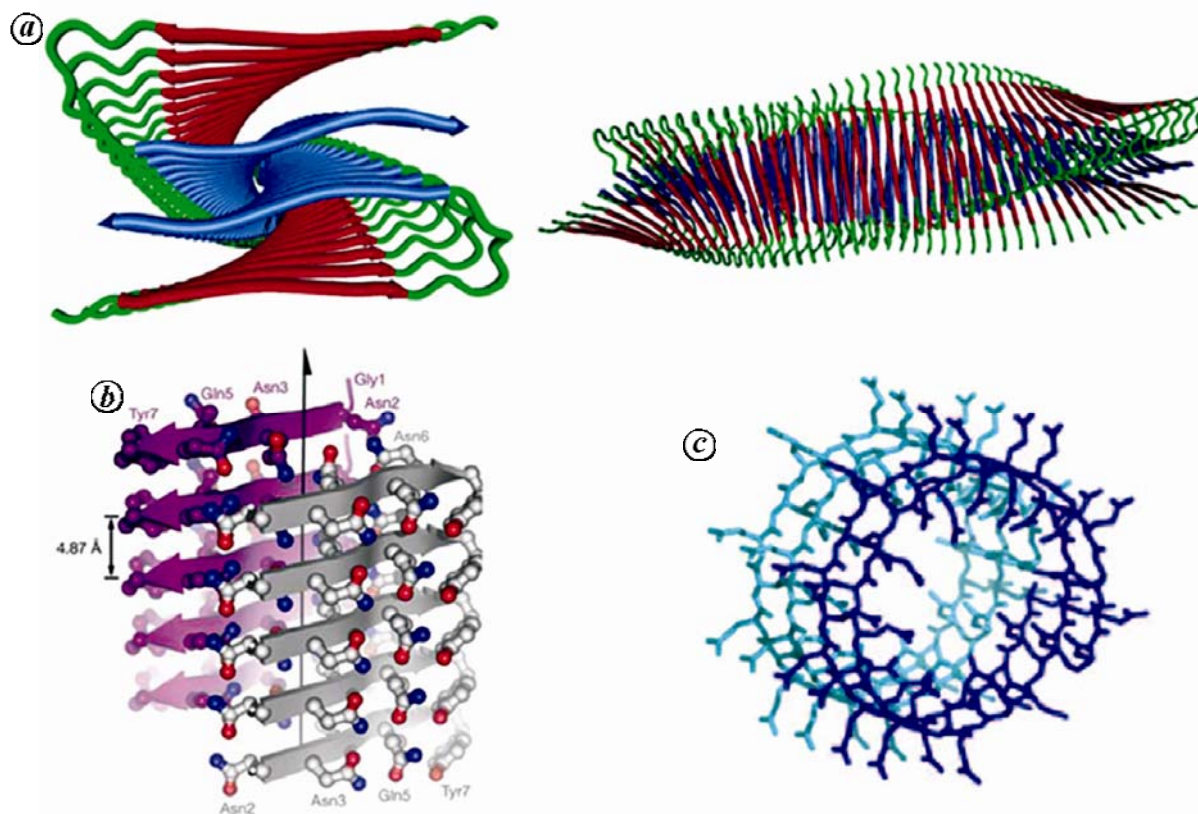
Figure 1. Structural models of amyloid fibrils. *a*, Ribbon diagram of an amyloid-β_{1-40} protofilament, as viewed parallel (left panel) and perpendicular (right panel) to the fibril axis. This structural model is based on solid-state NMR data combined with constraints from electron microscopy data. Each Aβ molecule contributes two β-strands in the parallel β-sheets. Reprinted with permission from Petkova *et al.*[44]. *b*, Steric zipper, the cross-β motif in the fibrils of GNNQQNY. Each arrow represents the backbone of the β-strand. The side chains from the two β-strands intercalate to form a dry interface between them. Reprinted with permission from Nelson *et al.*[47]. *c*, β-helix structure of polyglutamine (PolyQ) fibrils[50]. A stick model of two stacked subunits of Q_{42} is shown. Reprinted from Singer and Dewji[51].

to be prevalent in the assembly intermediates formed at initial times of the reaction[37–39]. This review critically examines current knowledge and understanding of the mechanisms of amyloid fibril formation, the structural heterogeneity inherent in the process, as well as the role of structural heterogeneity in determining how fibrils form. The current molecular level understanding of the structural heterogeneity in amyloid fibrils is also discussed.

Structure of amyloid fibrils

Amyloid fibrils are ~10 nm in their diameters, and are composed typically of 2–6 protofilaments. Amyloid fibrils of all proteins possess the same structural motif, the cross-β motif, wherein the β-strands are oriented perpendicular to, and the β-sheets parallel to the fibril axis[20,21,40]. In cross-β motifs, the separation between hydrogen-bonded β-strands is ~0.48 nm, and that between β-sheet layers is ~ 1.0–1.3 nm (ref. 41).

Understanding the molecular details of amyloid fibril structures has been a challenge owing to the large size,

the low solubility and the noncrystalline nature of fibrils. Recently, however, the use of solid-state NMR[42] has contributed to the considerable progress being made in the understanding of amyloid fibril structure. An elegant example is the structural model of the amyloid-β_{1-40} protofilament (Figure 1 *a*), which has been proposed on the basis of constraints from solid-state NMR studies, combined with measurements of fibril dimensions and of the mass-per-length (MPL) from electron microscopy images[43,44]. In this model, the first 10 residues of amyloid-β_{1-40} molecule are in a disordered conformation. Residues 12–24 and 30–40 form the core region of the fibrils, and exist in a β-strand conformation. The two β-strands of each amyloid-β_{1-40} molecule are connected via a bend region containing residues 25–29, and are parts of two distinct in-register, parallel β-sheets interacting through their side chains in the same protofilament. This suggests that a single cross-β unit consists of a double-layered β-sheet structure. A single amyloid-β_{1-40} protofilament appears to comprise two cross-β motifs, i.e. four β-sheets with an intersheet distance of ~1 nm. This structural model of amyloid-β_{1-40} amyloid fibrils is consistent

with studies by other methods, such as X-ray fibre diffraction, electron paramagnetic resonance, hydrogen-exchange and proteolysis[45]. Solid-state NMR and electron microscopy experiments have suggested that the fibrils formed by amyloid-β_{1-42} have similar supramolecular structures[46].

Our understanding of amyloid fibril structure has improved greatly by recent X-ray structure determinations of microcrystals of the amyloid-forming segments of 10 different amyloidogenic proteins[47,48]. As suggested earlier[43,49], these studies indicate that the cross-β motifs in amyloid fibrils formed by these amyloidogenic segments consist of a pair of β-sheets. Three levels of organization are apparent. The first level of organization represents a β-sheet formed by the alignment of the peptide fragments. In the second level of organization, two such β-sheets self-complement to form a pair of sheet structures, in which the side chains protruding from the two sheets intercalate to form a dry 'steric zipper' (Figure 1 b). In the third level of organization, interactions between the pairs of sheet structures lead to the formation of amyloid fibrils.

In the case of polyglutamine fibrils, it has been proposed that β-helices, structures significantly different from the classical amyloid fibrils, are generated by the involvement of additional hydrogen bonds between the side chains[50,51]. These structures could be cylindrical β-sheets of 3.1 nm diameter with 20 residues per helical turn. In this cylinder, the neighbouring turns are linked by hydrogen bonds between backbone amides as well as by those between side-chain amides, and the side chains point alternatively in and out of the cylinder (Figure 1 c).

In contrast to our knowledge of mature amyloid fibrils, very little is known about the internal structures of amyloid protofibrils. These are curly and elongated nano-structures, which sometimes appear to circularize into annular protofibrils (see below), and which are seen to form at initial times of fibril formation by many proteins. Several studies utilizing fluorescence spectroscopy[52], Fourier-transform infrared (FTIR) spectroscopy[53] or HX-MS[54] have all suggested an increase in internal order from soluble oligomers to protofibrils to fibrils. The thioflavin T binding ability as well as the β-sheet content of protofibrils is seen to be less than those of mature fibrils[55]. In the case of the amyloid-β protein[54], HX-MS has suggested that protofibrils possess β-sheet elements that extend to adjacent residues in mature fibrils. The internal organization of the β-sheets in protofibrils remains to be investigated by higher resolution structural probes.

Mechanisms of protein polymerization

The mechanism of polymerization of cytoskeletal proteins and sickle cell haemoglobin has been studied in great detail, and has been described in terms of two basic models[56–59], namely, nucleation-dependent polymerization and isodesmic (linear) polymerization. Since the data on protein aggregation reactions leading to protofibril and fibril formation are often evaluated in terms of these models, we first describe them briefly.

Nucleation-dependent polymerization

In a nucleation-dependent polymerization (NDP) reaction, the initial steps are slower than the later ones. A complete mathematical description of the kinetics of an NDP reaction requires forward and reverse rate constants for each step[60,61]. A simplifying strategy for analysis considers the initial steps to be close to equilibrium, and thus reduces the kinetic problem to an equilibrium one. From a thermodynamic viewpoint, an NDP reaction (Figure 2 a–e) can be described as follows. The initial steps (nucleation) consist of a number of unfavourable equilibria (Figure 2 a), that makes the initiation (nucleation) of polymerization difficult, and the system can be viewed as climbing an energy barrier which must be crossed for the polymerization to proceed (Figure 2 b). The peak of the free energy curve corresponds to a species (A_n in Figure 2 a) which marks a turning point in the polymerization reaction, after which downstream steps (elongation) become thermodynamically favourable. This high energy and thus very scarce species is the nucleus, and it constitutes a bottle neck in the polymerization reaction.

The slope of the free energy barrier (Figure 2 b) at any value of aggregate size is determined by the product of the concentration and the ratio of the association to dissociation rate constants[61]. In the nucleation phase (Figure 2 a and b), the dissociation rate constants are greater than the association rate constants. Once the nucleus is formed, the slope of the energy curve (Figure 2 b) reverses its direction, and for all the subsequent steps, the association rate constants become greater than the dissociation rate constants. Thus, in terms of the reaction kinetics, the nucleus represents the smallest protein aggregate for which the rate constant of association is greater than that of dissociation.

Characteristics of an NDP reaction

An NDP reaction has the following characteristics[61,62]. (1) The kinetics of polymer formation shows a lag phase. The lag time represents the weak initiation phase of the kinetics, and appears to be describable by a t^2 function (Figure 2 c and inset). The lag time in the kinetics of an NDP reaction arises because the dissociation rate constant is greater than the association rate constant in the initial part of the reaction (nucleation phase). The duration of the lag phase is proportional to the steepness of the energy curve in the initial part (Figure 2 b), and depends on protein concentration. The dependence of the
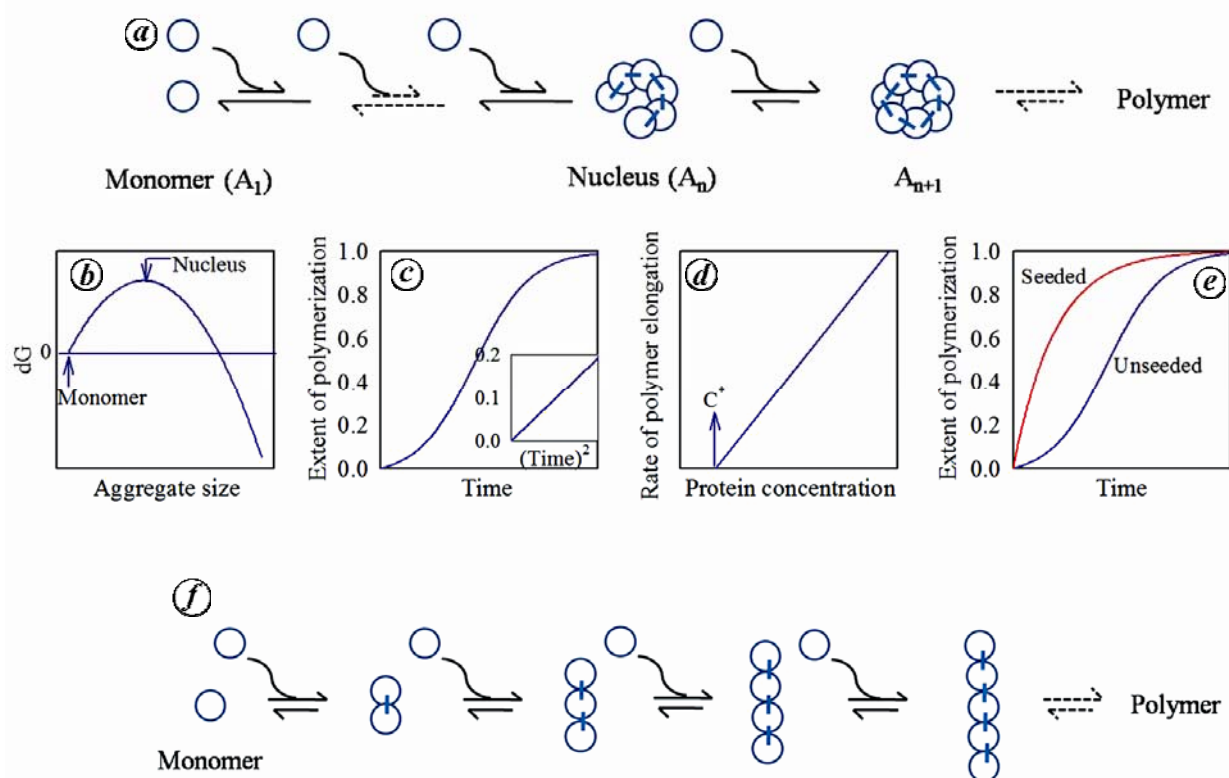
Figure 2. Protein aggregation reactions. *a*, Schematic of an NDP reaction showing nucleation and elongation phases. *b*, Free energy barrier in an NDP reaction. Panels *c–e* show the three characteristic kinetic features of an NDP reaction, namely, the presence of a lag phase (*c*); A critical concentration C* (*d*); Removal of the lag phase by seeding (*e*). *f*, Schematic of an isodesmic polymerization reaction.

lag time on protein concentration is controlled by the values of the association and dissociation rate constants as well as by the size of the nucleus (i.e. the number of monomers in the nucleus)[63]. (2) There is a critical concentration for the formation of polymer. The lag phase of an NDP reaction shows a strong dependence on protein concentration; the lag time increases with a decrease in protein concentration. This implies that at a sufficiently low monomer concentration, which would vary from protein to protein, no polymer will form. This characteristic monomer concentration is referred to as the critical concentration. At equilibrium, a finite amount of the monomer would exist in equilibrium with the polymer[62]. The critical concentration is usually determined from a plot of the rate of polymer formation (or amount of polymer) versus protein concentration (Figure 2 *d*). (3) The lag phase is abolished if a small amount of pre-formed nuclei (seed) is provided at the beginning of the reaction (Figure 2 *e*). This phenomenon is referred to as seeding.

Nucleation-dependent polymerization with secondary pathways

The theory of the NDP reaction successfully describes the kinetics of polymerization of many proteins. But in a few

cases, the kinetics of the increase in the amount of polymerized material is much more abrupt than that predicted by a t^2 dependence, and is better described as an exponential time dependence. To explain this exponential time dependence of polymerization kinetics, the theory of NDP reaction was extended to include secondary mechanisms of polymer formation[60,61], such as fragmentation[64,65], branching and heterogeneous nucleation[66].

Isodesmic (linear) polymerization

In an isodesmic (linear) polymerization reaction[56] (Figure 2 *f*), there is no separate nucleation and elongation phase[59,67]. Rather, polymerization can commence from any of the monomeric subunits. Each association step involves an identical bond, i.e. the rate constants are independent of the size of the polymer. Thus, an isodesmic polymerization reaction can be considered to be similar to the elongation phase of the NDP model. In the kinetics of an isodesmic polymerization reaction, no lag phase is seen, and the rate is fastest at the start of the reaction where the concentration of monomers is the highest; thereafter the rate decreases as the reaction proceeds towards equilibrium. There exists no critical concentration barrier.
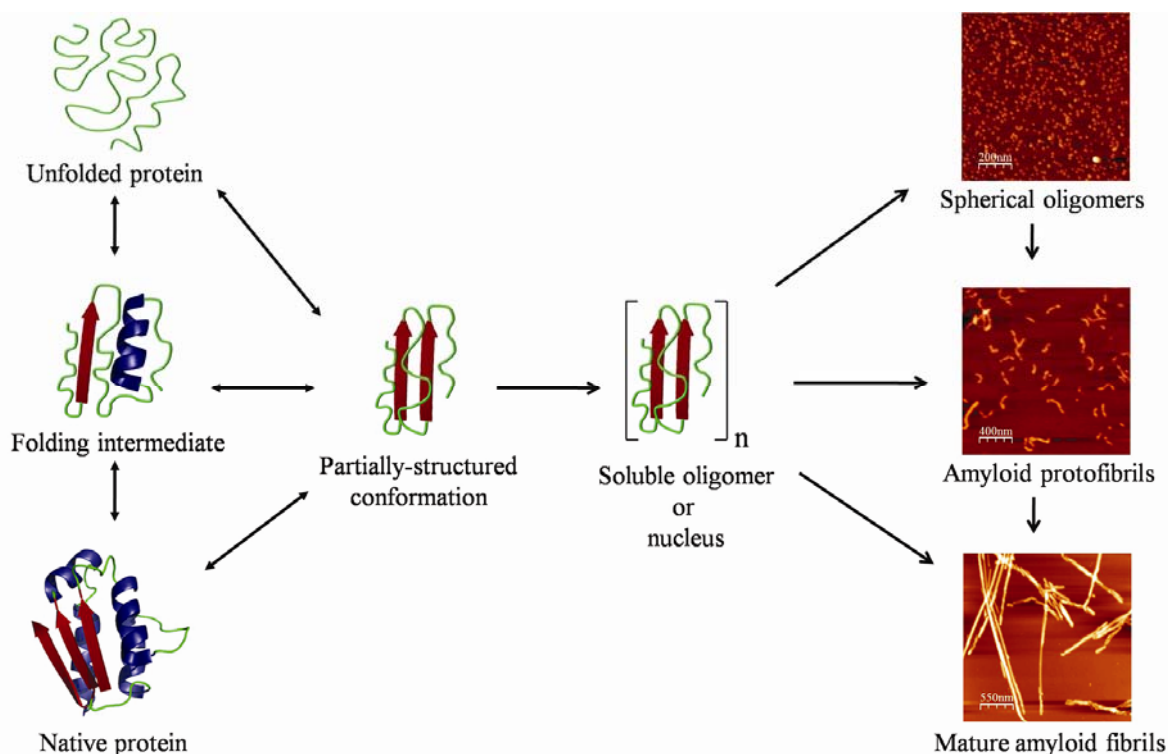
Figure 3. Protein folding and amyloid formation. Amyloid fibril formation commences from partially (un)folded conformers, which can form by partial unfolding of globular proteins, partial folding of natively unfolded proteins, or by conformational change in folding intermediates. These partially (un)folded amyloidogenic conformations self-assemble into amyloid fibrils. During the amyloid fibril formation reactions of many proteins, the conversion of partially (un)folded conformations into fibrils occurs through pre-fibrillar aggregates (spherical oligomers and/or protofibrils). The scale bars in the atomic force microscopy images of spherical oligomers, protofibrils and mature fibrils represent, respectively 200, 400 and 550 nm.

Establishing polymerization mechanisms by kinetic analysis

A polymerization reaction is considered to be nucleation-dependent if it shows all the three characteristic features of the NDP mechanism (see above). The features of the NDP reaction are prominent at lower protein concentrations. At very high protein concentrations, nucleation may, however, become relatively favourable, and the lag phase and the dependence on protein concentration of the kinetics may disappear[68].

Generally, an isodesmic polymerization reaction does not display any of the three characteristic features of an NDP reaction. But it is not always straightforward to distinguish between the two polymerization mechanisms, because the distinction between them is subtle, and rests solely on the nucleus size and the rate constants for dissociation and association. Under some circumstances, an isodesmic polymerization mechanism can readily mimic the features of the NDP mechanism. For a polymerization reaction to be considered as an NDP reaction, it needs to show all three characteristic features (see above), because an isodesmic polymerization reaction can show at least two of the three features[67]. Finally, it is important to realize that the NDP and isodesmic mechanisms represent two extreme cases of polymerization, and a given polymerization reaction may involve both the mechanisms at the same time[67].

Mechanism of amyloid fibril formation

Onset of amyloid fibril formation

The process of amyloid fibril formation seems to commence from partially structured conformers of proteins[69–71] (Figure 3). The partial (un)folding of proteins seems to facilitate specific intermolecular interactions, such as hydrophobic and electrostatic interactions, which are required to drive the polymerization of protein molecules into amyloid fibrils. But direct structural information on monomeric partially unfolded conformers competent to form amyloid fibrils, is available in only a few cases, because it is not easy to trap such partially unfolded conformers. Amyloid fibril formation by tetrameric transthyretin commences only after its dissociation into monomers[72], and the propensity to fibrillate is related inversely to the stability of the tetramer[73,74]. An HX-NMR study of monomeric transthyretin under amyloidogenic conditions suggested that the formation of the aggregation-competent intermediate is associated with the desta-

bilization of one of the β-sheets comprising the native fold[75]. Equilibrium unfolding measurements by NMR on a monomeric amyloidogenic conformation of β_2-microglobulin have suggested that the N-terminal region of the protein is predominantly unstructured, and that five of the seven β-strands comprising the native structure are retained in this species[76].

For most other proteins, there is only indirect evidence for the participation of partially unfolded conformations in amyloid formation. It has been shown for many proteins that the propensity to fibrillate is determined by, and is related inversely to, the stability of the protein[69,77-83]. Consequently, factors destabilizing the native fold of a protein tend to increase the propensity of the protein to fibrillate. Conversely, factors that stabilize the native fold of a protein are seen to reduce the fibril formation propensity of the protein[84]. Importantly, in the case of amyloid fibril formation by β-lactoglobulin, the aggregation propensity has been seen to be the highest at the urea concentration corresponding to the mid-point of unfolding transition of the protein[85].

Partial unfolding of proteins can be induced by mutations, by changes in environmental conditions or by chemical modifications. It is instructive to note that although the conformational transition of the native structure into a partially structured form seems to be a necessary step, amyloid fibril formation from a globular protein can occur under native conditions[86]. Amyloid fibril formation under native conditions would initiate from a locally unfolded segment of a globular protein, which becomes accessible, for example, during conformational breathing motions of the protein.

In the case of natively unfolded proteins (such as α-synuclein, amyloid-β protein, tau, etc.), the formation of partially structured conformers can occur by partial folding, and fibril formation is promoted by factors that induce partial folding[71,87,88]. For example, in the case α-synuclein, either a decrease in pH or an increase in temperature appears to induce partial folding, and to enhance the propensity of the protein to fibrillate[89].

Nucleation and growth (elongation) mechanisms

For some proteins, amyloid fibril formation appears to occur via the NDP mechanism, wherein the reaction appears to commence from oligomeric nuclei, which grow by the sequential addition of monomeric intermediates. The formation of amyloid fibrils by these proteins[85,90-96] involves an initial lag phase in the kinetics, which is eliminated upon seeding. But critical concentrations have been determined only in a few cases. It is important to note that in most fibril formation reactions showing features of the NDP mechanism, the kinetics show only weak dependences on protein concentration[93,97,98]. This has led to the conclusion that the nucleus size is small. In

the case of amyloid fibril formation by polyQ peptides, a very weak dependence of the lag time on protein concentration suggested a monomeric nucleus. Thus, an unfavourable conformational change in the monomeric protein seems to constitute the rate-determining nucleation event[99,100]. For some proteins, secondary nucleation events, such as nucleation on the surface of pre-existing fibrils and on exogenous impurities, have also been proposed[101-103]. In the case of fibril formation by the amyloid-β protein at low pH[104,105], it has been proposed that above a certain critical concentration, the peptide first forms micelles which give rise to fibril nuclei. Below the critical concentration, fibril formation is thought to nucleate predominantly on exogenous impurities.

It is increasingly being realized that for many proteins, models of NDP are not adequate for extracting information on the size of the nucleus from the protein concentration-dependence of the kinetics of amyloid fibril formation[98]. This is so because in many cases of amyloid fibril formation, a large population of pre-nuclear oligomers is formed and/or mechanical agitation is used to induce the reaction, both of which can diminish the protein concentration-dependence of the kinetics, and can therefore lead to an underestimation of the nucleus size. Thus, a reliable determination of the nucleus size requires refinements in the strategy for the analysis of the protein concentration-dependence of the aggregation kinetics[98].

In the case of amyloid fibril formation by many proteins, spherical oligomers and/or protofibrils are seen to form rapidly, and, in many cases, mature fibrils appear upon extended incubation[38,52,53,106-115]. This aggregation mechanism has been referred to as 'assembly via oligomeric intermediates'[38,107,116]. In this mechanism, it appears that the formation of the pre-fibrillar aggregates is not limited by an unfavourable nucleation event[111,114,115,117], and can be considered as isodesmic polymerization[117].

It is not easy to carry out kinetic measurements to show that pre-fibrillar aggregates such as protofibrils transform directly into long straight mature fibrils, because of the inherent heterogeneity in the process and because of the insoluble nature of mature fibrils. It is difficult to rule out the possibility that pre-fibrillar aggregates represent off-pathway species formed as independent entities. Indeed, protofibrils and fibrils form under different aggregation conditions for some proteins[93,94,115,118]. For some proteins, the aggregation reaction seems to cease at the level of oligomers and protofibrils, and not to proceed to typical mature fibrils[38,39,114,116,117]. Mature fibrils may form upon a change in the aggregation conditions[110].

Nevertheless, it appears that the pre-fibrillar aggregates lie on the direct pathway of fibril formation for some proteins. In the case of the NM segment of Sup35, kinetic measurements suggest that oligomers formed initially during the reaction assemble directly into fibrils[107]. In the

case of the amyloid-β protein too, there is evidence supporting an on-pathway role for the pre-fibrillar aggregates[55,119]. It has been suggested that the protofibrils of the amyloid-β protein grow into mature fibrils by monomer addition as well as by lateral association[120]. The former mechanism appears to predominate at low salt concentrations, and the latter mechanism at high salt concentrations. Some structural data also point to the on-pathway role of pre-fibrillar aggregates formed by the amyloid-β protein; the β-sheet elements comprising the mature fibrils appear to be present in the pre-fibrillar aggregates[54,113]. In such cases, amyloid fibril formation might nucleate by conformational changes in the oligomeric and/or protofibrillar intermediates[107,121], and mature amyloid fibrils might form by association of the oligomeric intermediates, by addition of the oligomeric intermediates on to protofibrils, or by end-to-end and lateral association of protofibrils.

Acquisition of β-sheet structure

It is important to determine when β-sheet conformational conversion occurs during amyloid fibril formation. In amyloid fibril formation reactions displaying the characteristic features of the NDP mechanism, and in most examples of assembly via oligomeric intermediates, the growth of aggregates and the acquisition of β-sheet structure seem to be coupled[107,114–116,122,123]. It appears that the associating units (monomers or oligomers) first add on to the ends of the growing aggregates, and then undergo the β-sheet conformational change. Recently, it has been seen for two proteins that amyloid fibril formation involves conformationally converted oligomeric intermediates, i.e. the β-sheet conformational change occurs in the oligomeric intermediates before they add on to the ends of the growing aggregates. In the case of amyloid fibril formation by the amyloid-β protein[113], the monomeric protein molecules undergo a large conformational change to form spherical oligomeric intermediates, early during fibril formation. A structural comparison, using solid-state NMR, with the mature fibrils suggested that the formation of this β-sheet rich oligomeric intermediate largely defines the conformational change associated with fibril formation, and that the oligomeric intermediates undergo supramolecular reassembly to form amyloid protofibrils and fibrils. In the case of amyloid protofibril formation by wild type barstar[114] as well as by many of its single cysteine-containing mutant variants[38], the β-sheet conformational change occurs after or concurrently with the growth (elongation) of spherical oligomeric intermediates into protofibrils. But for two of the single cysteine-containing mutant variants of barstar (Cys62 and Cys89), the β-sheet conformational change is seen to occur in the spherical oligomeric intermediates before they assemble to form protofibrils[38].

Structural heterogeneity in amyloid fibril formation reactions

It seems that multiple distinct fibrillar morphologies can be adopted by any individual protein, and that the formation of fibrils by many proteins is preceded by the accumulation of a range of aggregated pre-fibrillar states (Figure 4). Understanding the structural as well as the kinetic basis of the conformational polymorphism seen in amyloid fibril structures is a major goal of protein aggregation studies. Such an understanding is necessary for gaining an insight into the phenomenon of prion strains[124], wherein the same prion protein adopts a range of infectious conformations differing in their specificity and transmission barrier[125–128].

In this section, we first describe the structural heterogeneity seen in the structures of mature fibrils. We then discuss how an understanding of the initial and intermediate stages of amyloid fibril formation reactions can provide an insight into structural heterogeneity in mature fibrils.

Structural heterogeneity in mature amyloid fibrils

A protein may assemble into amyloid fibrils of multiple distinct morphologies in response to a change in amino acid sequence[129], upon a change in aggregation conditions[94,128,130,131], as well as under the same growth condition[112,132,133]. Multiple morphological variants, as seen by atomic force microscopy and electron microscopy[134], have been seen to differ in the number of protofilaments that comprise the mature fibrils as well as in the helicity of their intertwining[112,131,132]. In the assembly pathway of
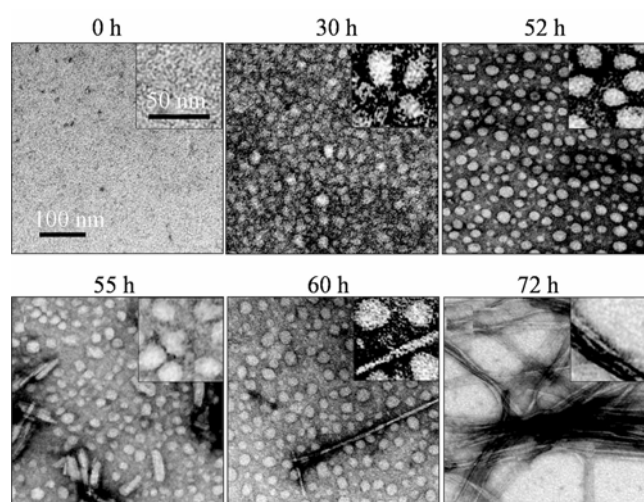

Figure 4. Morphologies of protein aggregates formed by the amyloid-$\beta_{1–40}$ protein after incubation for different times at pH 7.4, 4°C. Spherical oligomers and elongated protofibrils are seen to populate before the formation of mature amyloid fibrils. Spherical oligomers of a range of sizes are seen. Reprinted with permission from Chimon et al.[113].

the amyloid-β_{1-40} protein, spherical oligomers are formed at the initial times of the reaction, and subsequently polymorphic amyloid fibrils are formed upon prolonged incubation under the same conditions. Electron microscopy analysis has shown that the fibril polymorphs differ in their mass per length (MPL) values as well as in their axial cross-over spacing[106,112]. Two predominant morphologies have been identified. Amyloid fibrils in the MPL1 group have a MPL value of 18 ± 3 kDa/nm, and are multi-stranded cables with an axial cross-over spacing of ~25 nm. On the other hand, amyloid fibrils belonging to the MPL2 group have a MPL value of 27 ± 3 kDa/nm, and contain twisted ribbons with an axial cross-over spacing of ~80–130 nm, as well as multi-stranded cable morphologies. The amyloid-β_{1-42} protein is also seen to show fibril polymorphism with similar MPL values[46]. The morphologies of amyloid fibrils formed by amyloid-β_{1-40} and by amyloid-β_{1-42} are seen to be extremely sensitive to changes in aggregation conditions[46,131].

The β_2-microglobulin protein, including its deamidated variant, N17D, has been seen to form mature amyloid fibrils of three different morphologies[130,132], which differ in the number of protofilaments comprising them, as well as in the helicity of their intertwining. Type I and type II fibrils are multi-stranded cables with two and four protofilaments respectively, intertwined in a left-handed helical manner. Type III fibrils are twisted ribbons with four protofilaments arranged in a left-handed helical manner.

Under the same aggregation condition, calcitonin assembles into twisted ribbons, tubes and multi-stranded cables[135]. Amylin[136], transthyretin[137], α-synuclein[133], the prion proteins[125,128,138] and many other proteins have been seen to form amyloid fibrils of different types, as seen in atomic force microscopy and electron microscopy images.

The available data indicate that mature amyloid fibrils consist of multiple protofilaments, and are multi-stranded cables or twisted ribbons[36]. In such a case, amyloid fibril polymorphism can be explained by a simple model, wherein the same protofilaments assemble in diverse patterns to give rise to morphologically distinct amyloid fibrils of the same protein. The morphological polymorphs of amyloid fibrils have been seen, however, to differ in their underlying molecular structures. In the case of amyloid-β, a comparison of the two-dimensional solid-state ^{13}C NMR spectra of two morphological polymorphs, formed under two different aggregation conditions, suggested that they differ in their underlying molecular structures[131]. Interestingly, in the assembly reaction of α-synuclein, mature fibrils were seen to differ in their underlying internal structures, even though they were hardly distinguishable by their external morphologies[133].

Thus, it appears that the structural heterogeneity in amyloid fibrils might originate from variations in the internal structure of the cross-β motif. These variations might be in the nature and registry of the β-sheets, in the number of residues in the β-strands, as well as in the spacing between the β-sheets[11,46,139–143]. In addition, the presence and absence of disulphide bonds can affect the morphology of amyloid fibrils, perhaps by affecting the structure of the cross-β motif[144]. The X-ray structures of microcrystals of a number of amyloid-forming segments of amyloidogenic proteins[48] have shed further light on how the cross-β motif can show variations. The variations in the fundamental steric zipper structure of the cross-β motif may be in the orientation of the β-strands (parallel or antiparallel) within the sheets, in the orientation of the β-sheets (parallel or antiparallel) with respect to one another, or in the packing of the sheets (face-to-face or face-to-back).

Thus, differences in the nature of the amino acid side chains can lead to cross-β structures of distinct atomic architectures, and can explain atomic level variations in the structures of amyloid fibrils formed by different proteins and peptides, as well as those induced by protein mutations. It is interesting to note that several proteins possess more than one amyloidogenic segment, and that different segments of a protein can form amyloid fibrils of significantly different structures[48]. In such a scenario, polymorphism in the amyloid fibrils formed by a protein may originate in many ways. Amyloid fibril polymorphs of a protein may be formed by different segments or different combinations of the amyloidogenic segments of the protein. It is also possible that different amyloidogenic segments or different combinations of the segments of the protein are preferentially utilized for fibril formation under different aggregation conditions. This may explain the formation of structurally distinct amyloid fibrils by a protein under different environmental conditions. Alternatively, the formation of polymorphic fibrils under different aggregation conditions may arise purely from the effects of the different solvent conditions on the intermolecular interactions in the steric zipper formed by the same amyloidogenic segment of the protein.

Structural heterogeneity in partially (un)folded conformers

An important question is whether the partially structured conformers from which aggregation commences, represent multiple distinct sub-populations of conformations co-existing with one another. If there are multiple partially structured conformations, the aggregation reaction can potentially commence from many of them[145]. In order to understand the kinetic origin of the structural heterogeneity in amyloid fibrils, it is, therefore, important to identify structural heterogeneity in the partially structured conformations.

Partially structured conformations are populated by partial unfolding in the case of globular proteins. The use of high resolution probes, such as time-resolved fluorescence resonance energy transfer, or HX-MS and HX-

NMR, to monitor protein unfolding reactions is now increasingly making it evident that the unfolding reaction proceeds through many different partially unfolded conformations[146–149]. The partially unfolded conformations of proteins are heterogeneous, and different sub-populations may accumulate under different unfolding conditions.

Conversely, partially structured conformers can accumulate by partial folding in the case of natively unfolded proteins. It has been generally assumed that natively unfolded proteins exist in a denatured (random coil) state. It now appears that they exist not in random coil states, but in collapsed forms[67]. It seems reasonable to define two possible states of natively unfolded proteins: disordered-denatured and disordered-collapsed. Probably, only the disordered-collapsed states are capable of forming amyloids[67]. Polyglutamine[150], amyloid-β[151], α-synuclein[152] and the NM segment of the yeast prion protein Sup35[153] have all been shown to exist as ensembles of collapsed structures.

Structural heterogeneity in pre-fibrillar aggregates (spherical oligomers and protofibrils)

The initial phase of fibril formations by many proteins is characterized by the accumulation of spherical oligomers and protofibrils (Figure 4). Electron microscopy and atomic force microscopy experiments show that the earliest pre-fibrillar aggregates are spherical oligomers[38,52,53,107,108,111,114–117,132], which subsequently seem to coalesce to form beaded, elongated worm-like amyloid protofibrils. The elongated protofibrils may sometimes circularize to form annular, ring-like protofibrils[154–157]. Recently, the annular protofibrils of the amyloid-β protein were shown to differ structurally from spherical oligomers; they display an epitope that is absent in spherical oligomers and in fibrils of the protein[157]. Understanding the structural heterogeneity in these pre-fibrillar oligomers and protofibrils is crucial not only to gain an insight into the structural heterogeneity seen in the mature amyloid fibrils, but also because pre-fibrillar oligomers and protofibrils appear to represent the toxic species in amyloid-related diseases[113,158–160].

It now appears that heterogeneity exists within the individual sub-populations of pre-fibrillar aggregates. The pre-fibrillar oligomers are seen to be heterogeneous in size, and seem to consist of a continuum of oligomeric states[95,109,161–163]. The pre-fibrillar oligomers appear to show heterogeneity also in their secondary structure content[38,39,162]. In the case of protofibril formation by barstar at high temperatures[38], mutational analysis has revealed that the spherical oligomers formed initially in the reaction consist of two sub-populations, one rich in α-helix and another rich in β-sheet. Wild type barstar and many of its single cysteine-containing variants populate predominantly the spherical oligomers rich in α-helix,

whereas the spherical oligomers formed in the case of two of the mutant forms (Cys62 and Cys89) are predominantly β-sheet structures. Furthermore, the spherical oligomers formed during the trifluoroethanol (TFE)-induced aggregation of wild type barstar[39] appear to have a higher α-helical content than that of the spherical oligomers formed by the protein at high temperatures.

Annular protofibrils too appear to show structural heterogeneity. The spherical oligomers of wild type α-synuclein form annular protofibrils of two different morphologies differing in their heights, as seen by atomic force microscopy, as well as in their diameters[164]. Under the same aggregation conditions, the spherical oligomers of the A53T mutant variant of the protein form annular protofibrils having a diameter that is much smaller than that of the protofibrils formed by the wild type protein. Furthermore, the annular protofibrils formed by the wild type protein and by a 1:1 mixture of the wild type and the A53T mutant variant differ significantly in their heights on mica (1.3 nm for one of the polymorphs of the wild type protein, and 2.7 nm for the 1:1 mixture of the wild type protein and the A53T mutant form)[164].

Very little is known about structural heterogeneity in elongated protofibrils; nearly all information in this regard comes from studies on barstar aggregation[38,39]. The elongated protofibrils formed at high temperatures by the Cys62 and Cys89 mutant forms of barstar have thioflavin T binding abilities similar to those of the protofibrils formed by the wild type and many other mutant forms of the protein. Far-UV CD suggests, however, that the protofibrils formed by Cys62 and Cys89 have a lower β-sheet content. Atomic force microscopy experiments show that these polymorphs of heat-induced amyloid protofibrils of barstar differ in their heights on mica surfaces. The protofibrils formed by Cys62 and Cys89 have larger diameters, as determined from their heights in atomic force microscopy images, than those formed by the wild type and other mutant forms of the protein under the same conditions[38].

Heterogeneity in the amyloid protofibrils of barstar becomes more evident upon a change in aggregation conditions. The amyloid protofibrils of wild type barstar formed in the presence of TFE (TFE-induced protofibrils) differ from those formed at high temperatures (heat-induced protofibrils) in their external dimensions, in their internal structures, as well as in their stabilities[39] (Figure 5). The mean thickness of the TFE-induced protofibrils, as determined from the Z-heights in atomic force microscopy images, is about half the thickness of the heat-induced protofibrils (Figure 5 a and b). The thickness of the TFE-induced protofibrils (1.14 ± 0.24 nm) suggests that they consist of a β-sheet monolayer. In contrast, the thickness of the heat-induced protofibrils (2.56 ± 0.32 nm) suggests that they are composed of a pair (bilayer) of β-sheets. This result from the atomic force microscopy experiments is supported by stability meas-

urements and by dynamic light scattering experiments[39]. The presence of amyloid-like β-sheet structures in the TFE-induced and in the heat-induced protofibrils is evident from the presence of a peak in the 1615–1643 cm^{-1} region[165,166] in their FTIR spectra (Figure 5 *c* and *d*). Interestingly, the position of this peak for the TFE-induced protofibrils (1616 cm^{-1}) differs significantly from that seen for the heat-induced protofibrils (1621 cm^{-1}), which suggests that the β-sheets in the two differently generated protofibrils differ in their internal structures. Furthermore, the presence of a peak at 1650 cm^{-1} in the case of heat-induced protofibrils suggests that they are not pure β-sheet structures but that they also possess other structures[165,167] (helices and/or random coils). In contrast, the TFE-induced protofibrils do not show a peak at 1650 cm^{-1}, suggesting that they contain relatively more β-sheet structures, and less of other structures, if any. The far-UV CD spectra of the TFE-induced and heat-induced protofibrils are consistent with the structural differences pointed out by the FTIR spectra.

Multiple pathways of amyloid fibril formation: kinetic origin of amyloid polymorphism

Many lines of evidence suggest that protein mutations and changes in environmental conditions affect the kinetics of protein aggregation by affecting the stability of the native structure, as well as by changing the physicochemical properties (such as hydrophobicity, β-sheet propensity and charge) of the protein. The process of protein aggregation involves self-assembly through intermolecular interactions, and leads to an increase in β-sheet structure. This makes protein aggregation kinetics sensitive to changes in the above-mentioned physicochemical properties[168,169]. It is now becoming evident that the mechanism of protein aggregation reactions involves multiple assembly pathways. Protein mutations and changes in environmental conditions may affect the aggregation reaction by changing the aggregation pathway[38,39,94,109,112,129,170]. It is instructive to consider a few examples where the existence of multiple independent pathways has been proposed to underlie the structural heterogeneity in protein aggregates.

β_2-microglobulin

β_2-microglobulin forms protein aggregates of distinct morphologies under varying aggregation conditions[94]. Worm-like fibrils are formed at pH 3.5, in the presence of 200 mM NaCl. These fibrils resemble the protofibrils formed by many other proteins[38,39,112,114] in having flexible curly morphologies. But unlike protofibrils which are typically <600 nm in length, worm-like fibrils can be much longer. Rod-like fibrils form at the same pH but at lower NaCl concentration (≤50 mM), and they seem to represent intermediates in the formation of the worm-like fibrils. It appears that the worm-like fibrils are dead-end products, and cannot be converted into mature amyloid fibrils. At pH < 3 and at low salt concentration[94,132,171], β_2-microglobulin forms long straight fibrils.

HX-NMR studies have suggested that conformational heterogeneity exists in the worm-like and in the long straight fibrils; the environment of some residues appears to vary from molecule to molecule[27,28]. The β-sheet core region in the worm-like and in the long straight fibrils appears to be formed by the central region of the protein molecule. But the β-sheet core spans a narrower region in the worm-like fibrils than in the long straight fibrils[27,28].

The kinetics of the formation of rod- and worm-like fibrils is monophasic without a lag phase[171]. A mass spectrometry study indicates that the formation of these fibrils involves a range of oligomeric states[95], suggesting that the reaction occurs in a progressive, non-cooperative manner. It appears that the formation of rod- and worm-like fibrils follows the isodesmic mechanism, and is not limited by an unfavourable nucleation event[94,95,171].

In contrast to the kinetics of the formation of rod-like and worm-like fibrils, the kinetics of the formation of long straight fibrils is sigmoidal with an initial lag phase. The duration of the lag phase reduces upon seeding[172]. Mass spectrometry studies indicate that the reaction does not involve stable higher order oligomeric or protofibril-
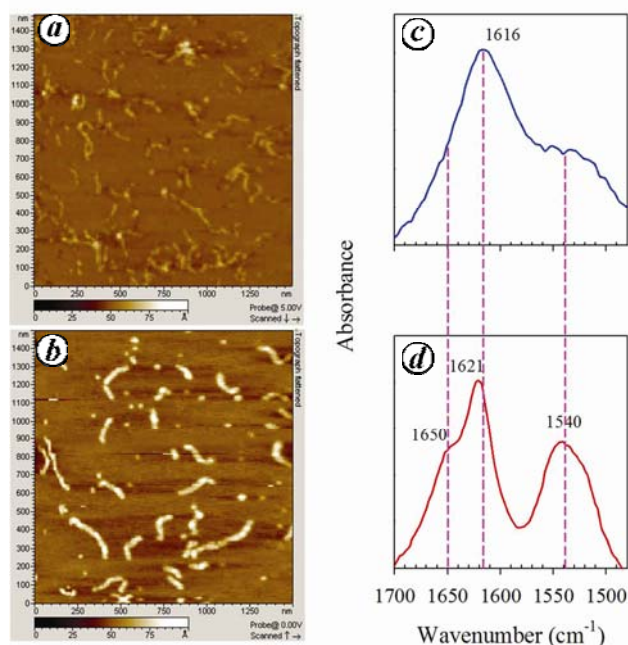

Figure 5. Structural characterization of TFE-induced and heat-induced protofibrils of barstar. *a*, Atomic force microscopy image of TFE-induced protofibrils. *b*, Atomic force microscopy image of heat-induced protofibrils. *c*, FTIR spectrum of TFE-induced protofibrils. *d*, FTIR spectrum of heat-induced protofibrils. Reprinted from Kumar and Udgaonkar[39].

lar intermediates[95]. It therefore appears that the formation of long straight fibrils occurs via a nucleation-dependent reaction. The critical concentration has, however, not been determined.

Mouse prion protein

In the case of the recombinant mouse prion protein (moPrP), an α-helix rich monomer (α-monomer) of the protein exists in equilibrium with oligomers rich in β-structures (β-rich oligomers)[115,173]. The equilibrium appears to be shifted towards the α-monomer at neutral pH, and towards the β-rich oligomers at acidic pH[174].

The available data indicate the existence of two pathways for the formation of amyloid fibrils by the moPrP. One pathway (at pH 7) commences from the α-monomer, and culminates in long straight fibrils in a reaction that appears to be nucleation dependent[173]. The kinetics of formation of these fibrils is sigmoidal with an initial lag phase, which is reduced upon seeding[97]. The kinetics is, however, only weakly dependent on protein concentration[97]. On the other pathway (at pH 2) the reaction starts from the β-rich oligomers, and leads to the formation of worm-like fibrils[115]. The kinetics of worm-like fibril formation is monophasic without a lag phase[115]. In this respect, the aggregation reaction of moPrP at low pH appears remarkably similar to that of β_2-microglobulin. In both cases, a monomer leads to the formation of long straight fibrils in an apparently nucleation-dependent manner, whereas an oligomer leads to the formation of worm-like fibrils in a reaction that does not seem to be limited by an unfavourable nucleation event.

Worm-like fibrils are seen to form only at low pH because the β-rich oligomer, from which they arise, is stable at low pH. At higher pH values, the stability of the β-rich oligomer reduces, presumably because of the deprotonation of a few critical residue side-chains. At pH 7, the concentration of the β-rich oligomer, which is competent to form worm-like fibrils, is so small that the formation of worm-like fibrils cannot be observed. Moreover, the rate of formation of worm-like fibrils will be extremely slow because the concentration of the β-rich oligomer is very low[115]. If the worm-like fibrils are indeed the toxic species, as are the smaller protofibrils formed by other proteins[113,158–160], then the late-onset of prion diseases could be explained by an extremely slow aggregation reaction whose rate is limited by the extremely low concentration of β-rich oligomer formed at the normal pH prevalent in cells.

Barstar

The small protein barstar forms soluble oligomers (the A form) at low pH. The A form is seen to be a symmetrical aggregate formed by 16 monomeric subunits of the protein[175,176]. NMR experiments have shown that the core of the A form consists of the C-terminal segments of the self-assembled monomeric units, and that the N-terminal segments are in random coil conformations[177]. In a process that is accelerated at higher temperatures, the A form converts into amyloid protofibrils, and upon extended incubation, into mature fibrils[38,52,110,114]. The transition from protofibrils to mature fibrils is slow, and is accelerated in the absence of salt[110].

Time-resolved fluorescence studies suggest that the cores of the aggregates in the A form and in the protofibrils formed at high temperature are similar, indicating that the A form acts as the direct precursor[52]. Dynamic light scattering and atomic force microscopy experiments suggest that early during the aggregation process, the A form completely converts into spherical higher oligomeric intermediates (HOIs), which then assemble further into protofibrils in a progressive manner[38,114]. The spherical HOIs represent the predominant aggregates visible in atomic force microscopy images at early times of aggregation. The beaded appearance of protofibrils seen at the completion of the reaction suggests that they have assembled directly from the HOIs. Furthermore, the rate of the transformation of the A form into protofibrils depends on the probe used to monitor the reaction.

Cysteine-scanning mutagenesis studies identify two classes of mutant proteins, which use structurally distinct pathways to form amyloid protofibrils[38]. The majority of mutant proteins follow Pathway I (Figure 6 a), where the A form first converts into HOIs which then grow in size to form the elongated protofibrils. Like for many other proteins, including wild type barstar (see above), β-sheet conformational change on this pathway occurs along with, or after elongation of the oligomers. Interestingly, on Pathway II (Figure 6 b), conformational change precedes elongation of the oligomers. The A form first transforms into HOIs. The HOIs undergo β-sheet conformational conversion to form conformationally converted HOIs (CC-HOIs), which then assemble to form elongated protofibrils. On both the pathways, the mean hydrodynamic radius-monitored kinetics are significantly faster that the kinetics monitored by scattering intensity, suggesting that elongated protofibrils associate laterally to form the mature amyloid protofibrils[178]. The amyloid protofibrils formed on these alternative pathways differ in their structures.

A comparison of amyloid protofibril formation by wild type barstar under two different growth conditions, one in the presence of TFE and the other at high temperature, reveals that the pathway of TFE-induced protofibril formation is distinct from that of heat-induced protofibril formation[39] (Figure 6 a and c). The kinetics of heat-induced protofibril formation is monophasic; no lag phase is seen. The kinetics shows a weak dependence on protein concentration, and there is no apparent critical concentration. It appears therefore that the heat-induced formation of protofibrils follows the isodesmic (linear)
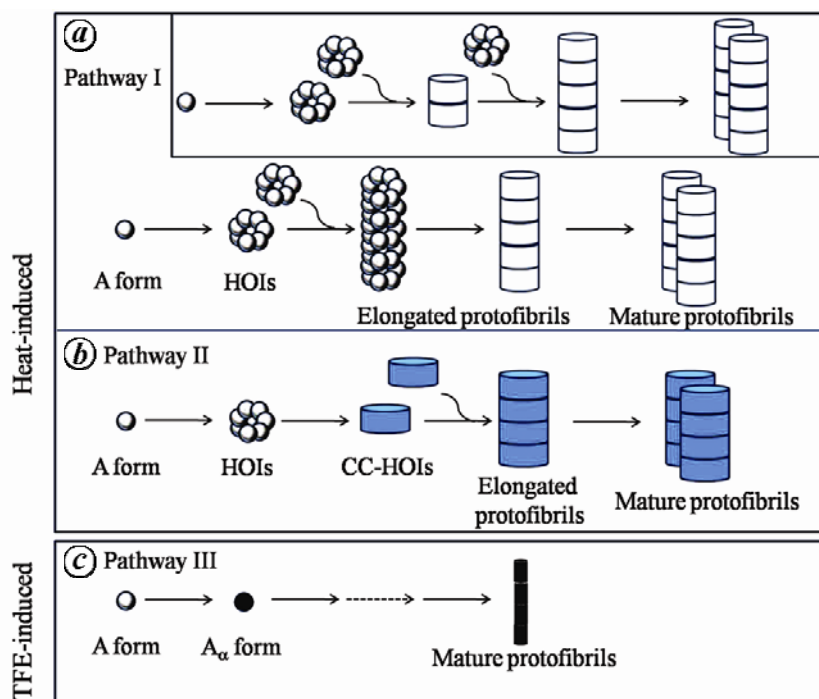
Figure 6. Multi-pathway mechanism for amyloid protofibril formation by barstar. Pathways I and II operate in the case of heat-induced protofibril formation, while TFE-induced protofibril formation occurs via Pathway III. *a*, Pathway I: The A form is first converted into higher order oligomeric intermediates (HOIs) which then grow in size to form the elongated protofibrils. The conformational conversion leading to the formation of thioflavin T-binding sites and increase in β-sheet content seems to occur within these elongated protofibrils. The inset brings out the possibility that conformational conversion may occur concurrently with growth (elongation). *b*, Pathway II (assembly via conformationally converted oligomers): the A form is first converted into HOIs which undergo conformational conversion to form conformationally converted HOIs (CC-HOIs), which then assemble to form the elongated protofibrils. On both the pathways, the elongated protofibrils then seem to associate laterally to form the mature amyloid protofibrils. *c*, Pathway III: TFE-induced protofibril formation commences from the A_α form. No lateral association of elongated protofibrils appears to occur on this pathway. The amyloid protofibrils formed on these alternative pathways differ in their structures. Adapted from Kumar and Udgaonkar[38,39].

mechanism. In contrast, TFE-induced protofibril formation appears to be cooperative, with a distinct lag phase followed by an elongation phase. TFE-induced formation of protofibrils displays two of the three defining features of the NDP mechanism: the kinetics show a lag phase and the lag phase is reduced upon seeding. But the kinetics is only weakly dependent on protein concentration, and seeding has only a weak effect on the kinetics. The TFE-induced reaction does not show the third defining feature of the NDP mechanism; a critical concentration, below which no aggregation occurs, is not observed. Hence, TFE-induced protofibril formation cannot be described as an NDP reaction. As discussed above, the lag phase in the TFE-induced protofibril formation can also be described by the isodesmic mechanism. Thus, it is possible that TFE-induced protofibril formation involves both the NDP and isodesmic mechanisms (see above).

Unlike the heat-induced reaction, where the A form acts as the direct precursor[38,114] (see above), the TFE-induced formation of amyloid protofibrils seems to commence from a structurally distinct A_α form, which accumulates immediately after the addition of TFE to the A form. The TFE-induced formation of amyloid protofibrils involves therefore a pathway that is different from that of heat-induced protofibril formation. Furthermore, unlike the heat-induced pathway, the TFE-induced pathway does not appear to involve a lateral association step. Not surprisingly, the protofibrils formed on the TFE-induced and heat-induced pathways are structurally distinct.

The data for barstar show that the spherical oligomers (HOIs) as well as the elongated protofibrils of barstar show structural polymorphism. The use of multiple structural probes to monitor the kinetics has suggested that the formation of distinct protofibril conformations occurs via alternative pathways. Single mutations and changes in the growth conditions can switch the aggregation reaction between alternative pathways, and can thereby lead to the formation of amyloid protofibrils of different structures.

Amyloid-β protein

The amyloid-β protein transiently forms oligomers of varying sizes, as well as protofibrils. Upon prolonged

incubation, polymorphic amyloid fibrils form[109,112,179–181]. Protofibrils are typically of ~6 nm height in atomic force microscopy images, up to ~600 nm in length, and have a MPL of 19 ± 2 kDa/nm (ref. 112). Two predominant populations of amyloid fibril polymorphs have been identified[112]. The MPL value of one of the polymorphs is seen to be 18 ± 3 kDa/nm. The morphology of these fibrils differs from that of the protofibrils, but their MPL value is identical to that of the protofibrils. This suggests, but does not prove that these fibrils form by a conformational change and subsequent elongation of protofibrils. The other fibril polymorph has an MPL of 27 ± 3 kDa/nm. The MPL of these fibrils is ~1.5-fold higher than that of the protofibrils, which suggests that they do not arise either from conformational change in protofibrils or from lateral association of protofibrils. Instead, it appears that these fibrils form by an independent mechanism. The growth rate of these fibrils is seen to be ~15-fold faster than that of protofibrils. The difference between the values of the MPLs of the two polymorphs suggests that the fibrils of the amyloid-β protein are built from *bona fide* elementary protofilaments of an MPL of ~9 kDa/nm. No fibrillar morphology corresponding to an MPL of 9 kDa/nm is, however, seen to populate during the reaction. It can be argued that the proposed concurrent multiple assembly pathways involve the same sequence of events to form the common *bona fide* elementary protofilaments, and differ only in the last step wherein the protofilaments assemble in distinct ways leading to the formation of fibrils of distinct morphologies. But it has been shown in an independent study[131] that distinct amyloid-β fibril morphologies differ in their underlying molecular structures. These data for amyloid-β suggest that polymorphism in the mature fibrils originates from the utilization of alternative aggregation pathways, probably arising from heterogeneity in the pre-fibrillar aggregates[109,182].

The kinetics of mature fibril formation by the amyloid-β protein displays an initial lag phase, which is shortened upon seeding[106,112]. It appears therefore that the formation of mature fibrils by the amyloid-β protein involves nucleation-dependent polymerization. Nucleation-dependent aggregation is expected to be cooperative and to proceed without any accumulation of stable pre-fibrillar oligomers[93,95,99]. But the formation of mature fibrils by amyloid-β is seen to be preceded by the accumulation of spherical oligomers and protofibrils[112,113]. Thus, it appears that the fibril formation mechanism by amyloid-β is much more complex than that expected from either the isodesmic or the nucleation-dependent mechanism.

Polyglutamine (polyQ)-containing proteins and peptides

Simple polyQ peptides have been seen to form amyloid fibrils in a nucleation-dependent mechanism, and no oligo-meric and protofibrillar intermediate species have been seen to accumulate during the reaction[99,100,183]. The addition of a proline-rich sequence[184] to the C-terminus of the polyQ peptide decreases the rate of aggregation and the stability of the fibrils, but the fundamental mechanism of fibril formation appears to remain the same. The addition of oligo-proline sequences to the N-terminus of the peptide has no effect on the aggregation reaction. Recently, it was shown that the addition of HTT^{NT} (a 17 amino acid sequence from the huntingtin exon 1 fragment) to polyQ peptides leads to a complex alternative fibril formation mechanism[170]. In contrast to the fibril formation reaction by simple polyQ, where the earliest observable aggregates are fibrillar, fibril formation by HTT^{NT}-containing polyQ appears to occur via oligomeric and protofibrillar intermediates, and the reaction does not seem to be limited by an unfavourable nucleation event.

Conclusion

The energy landscape describing the process of protein aggregation is complex. There seems to be many energy minima, each representing a distinct amyloid fibril or protofibril conformation. Considerable progress has been made towards understanding the structural basis of amyloid fibril polymorphism, and an important goal of protein aggregation studies is to understand the kinetic basis of amyloid fibril polymorphism. The existence of structural heterogeneity in the partially structured precursor conformations and in pre-fibrillar aggregates suggests that the formation of fibrils may nucleate from a number of distinct precursor states, and many distinct elongation (growth) mechanisms might exist. Alternative pathways of amyloid fibril formation arising from heterogeneity in the nucleation and elongation mechanisms might lead to the formation of structurally distinct fibrils. One way by which this can occur is if distinct amyloidogenic segments of the protein are utilized on different pathways of amyloid fibril formation. Alternatively, different conformational sub-populations of the same amyloidogenic segment may be utilized on alternative pathways of fibril formation. *In vitro* experiments are now providing insights into the kinetic origin of amyloid fibril polymorphism. Amyloid fibril polymorphism can be understood in terms of the heterogeneity seen in partially structured aggregation-competent conformers as well as that seen in the pre-fibrillar aggregates. Such an understanding not only uncovers possible pathways of amyloid formation, but also suggests ways of modulating the pathways, and thus might provide insight into possible therapies for amyloid-related cell toxicity.

1. Allison, A. C., The role of microfilaments and microtubules in cell movement, endocytosis and exocytosis. *Ciba Found Symp.*, 1973, **14**, 109–148.

2. Singh, S., Koke, J. R., Gupta, P. D. and Malhotra, S. K., Multiple roles of intermediate filaments. *Cytobios*, 1994, **77**, 41–57.

3. Kunda, P. and Baum, B., The actin cytoskeleton in spindle assembly and positioning. *Trends Cell Biol.*, 2009, **19**, 174–179.

4. Silow, M. and Oliveberg, M., Transient aggregates in protein folding are easily mistaken for folding intermediates. *Proc. Natl. Acad. Sci. USA*, 1997, **94**, 6084–6086.

5. Silow, M., Tan, Y. J., Fersht, A. R. and Oliveberg, M., Formation of short-lived protein aggregates directly from the coil in two-state folding. *Biochemistry*, 1999, **38**, 13006–13012.

6. Ganesh, C., Zaidi, F. N., Udgaonkar, J. B. and Varadarajan, R., Reversible formation of on-pathway macroscopic aggregates during the folding of maltose binding protein. *Protein Sci.*, 2001, **10**, 1635–1644.

7. Wani, A. H. and Udgaonkar, J. B., HX-ESI-MS and optical studies of the unfolding of thioredoxin indicate stabilization of a partially unfolded, aggregation-competent intermediate at low pH. *Biochemistry*, 2006, **45**, 11226–11238.

8. Cromwell, M. E. M., Hilario, E. and Jacobson, F., Protein aggregation and bioprocessing. *AAPS J.*, 2006, **8**, E572–E579.

9. Fink, A. L., Protein aggregation: folding aggregates, inclusion bodies and amyloid. *Folding Design*, 1998, **3**, R9–R23.

10. Selkoe, D. J., Folding proteins in fatal ways. *Nature*, 2003, **426**, 900–904.

11. Chiti, F. and Dobson, C. M., Protein misfolding, functional amyloid, and human disease. *Annu. Rev. Biochem.*, 2006, **75**, 333–366.

12. Fowler, D. M., Koulov, A. V., Alory-Jost, C., Marks, M. S., Balch, W. E. and Kelly, J. W., Functional amyloid formation within mammalian tissue. *PLoS Biol.*, 2006, **4**, 100–107.

13. Scheibel, T., Parthasarathy, R., Sawicki, G., Lin, X., Jaeger, H. and Lindquist, S. L., Conducting nanowires built by controlled self-assembly of amyloid fibers and selective metal deposition. *Proc. Natl. Acad. Sci. USA*, 2003, **100**, 4527–4532.

14. Hamada, D., Yanagihara, I. and Tsumoto, K., Engineering amyloidogenicity towards the development of nanofibrillar materials. *Trends Biotechnol.*, 2004, **22**, 93–97.

15. Hamedi, M., Herland, A., Karlsson, R. H. and Inganäs, O., Electrochemical devices made from conducting nanowire networks self-assembled from amyloid fibrils and alkoxysulfonate PEDOT. *Nano Lett.*, 2008, **8**, 1736–1740.

16. Virchow, R., Zur cellulose-frage. *Virchows Arch. Pathol. Anat.*, 1854, **6**, 416–426.

17. Virchow, R., Ueber den Gang der amyloiden degeneration. *Virchows Arch. Pathol. Anat.*, 1855, **8**, 364–368.

18. Friedreich, N. and Kekule, A., Zur amyloidfrage. *Virchows Arch. Pathol. Anat.*, 1859, **16**, 50–65.

19. Hanssen, O., Ein Beitrag zur chemie der amyloiden entartung. *Biochem. Z.*, 1908, **13**, 185–198.

20. Eanes, E. D. and Glenner, G. G., X-ray diffraction studies on amyloid filaments. *J. Histochem. Cytochem.*, 1968, **16**, 673–677.

21. Sunde, M., Serpell, L. C., Bartlam, M., Fraser, P. E., Pepys, M. B. and Blake, C. C. F., Common core structure of amyloid fibrils by synchrotron X-ray diffraction. *J. Mol. Biol.*, 1997, **273**, 729–739.

22. Puchtler, H., Sweat, F. and LeVine, M., On the binding of congo red by amyloid. *J. Histochem. Cytochem.*, 1962, **10**, 355–364.

23. Klunk, W. E., Jacob, R. F. and Mason, R. P., Quantifying amyloid by congo red spectral shift assay. *Methods Enzymol.*, 1999, **309**, 285–305.

24. Naiki, H., Higuchi, K., Hosokawa, M. and Takeda, T., Fluorometric determination of amyloid fibrils *in vitro* using the fluorescent dye, thioflavin T. *Anal. Biochem.*, 1989, **177**, 244–249.

25. LeVine 3rd, H., Quantification of β-sheet amyloid fibril structures with thioflavin T. *Methods Enzymol.*, 1999, **309**, 274–284.

26. Kheterpal, I., Zhou, S., Cook, K. D. and Wetzel, R., Aβ amyloid fibrils possess a core structure highly resistant to hydrogen exchange. *Proc. Natl. Acad. Sci. USA*, 2000, **97**, 13597–13601.

27. Hoshino, M., Katou, H., Hagihara, Y., Hasegawa, K., Naiki, H. and Goto, Y., Mapping the core of the β2-microglobulin amyloid fibril by H/D exchange. *Nat. Struct. Mol. Biol.*, 2002, **9**, 332–336.

28. Yamaguchi, K., Katou, H., Hoshino, M., Hasegawa, K., Naiki, H. and Goto, Y., Core and heterogeneity of β2-microglobulin amyloid fibrils as revealed by H/D exchange. *J. Mol. Biol.*, 2004, **338**, 559–571.

29. Kheterpal, I., Williams, A., Murphy, C., Bledsoe, B. and Wetzel, R., Structural features of the Aβ amyloid fibril elucidated by limited proteolysis. *Biochemistry*, 2001, **40**, 11757–11767.

30. Frare, E., Mossuto, M. F., Polverino de Laureto, P., Dumoulin, M., Dobson, C. M. and Fontana, A., Identification of the core structure of lysozyme amyloid fibrils by proteolysis. *J. Mol. Biol.*, 2006, **361**, 551–561.

31. Sipe, J. D., The β-pleated sheet conformation and protein folding: a brief history. In *Amyloid Proteins: The Beta Sheet Conformation and Disease*, Wiley-VCH Verlag GmbH & Co. KGaA, Weinheim, Germany, 2005, pp. 49–61.

32. Finkelstein, A. V. and Ptitsyn, O. B., Secondary structures of polypeptide chains. In *Protein Physics: A Course of Lectures*, Academic Press, 2002, pp. 103–116.

33. Richardson, J. S. and Richardson, D. C., Natural β-sheet proteins use negative design to avoid edge-to-edge aggregation. *Proc. Natl. Acad. Sci. USA*, 2002, **99**, 2754–2759.

34. Wang, W. and Hecht, M. H., Rationally designed mutations convert de novo amyloid-like fibrils into monomeric β-sheet proteins. *Proc. Natl. Acad. Sci. USA*, 2002, **99**, 2760–2765.

35. Chiti, F., Webster, P., Taddei, N., Clark, A., Stefani, M., Ramponi, G. and Dobson, C. M., Designing conditions for *in vitro* formation of amyloid protofilaments and fibrils. *Proc. Natl. Acad. Sci. USA*, 1999, **96**, 3590–3594.

36. Kreplak, L. and Aebi, U., From the polymorphism of amyloid fibrils to their assembly mechanism and cytotoxicity. *Adv. Protein Chem.*, 2006, **73**, 217–233.

37. Kodali, R. and Wetzel, R., Polymorphism in the intermediates and products of amyloid assembly. *Curr. Opin. Struct. Biol.*, 2007, **17**, 48–57.

38. Kumar, S. and Udgaonkar, J. B., Conformational conversion may precede or follow aggregate elongation on alternative pathways of amyloid protofibril formation. *J. Mol. Biol.*, 2009, **385**, 1266–1276.

39. Kumar, S. and Udgaonkar, J. B., Structurally distinct amyloid protofibrils form on separate pathways of aggregation of a small protein. *Biochemistry*, 2009, **48**, 6441–6449.

40. Sunde, M. and Blake, C. C. F., From the globular to the fibrous state: protein structure and structural conversion in amyloid formation. *Q. Rev. Biophys.*, 1998, **31**, 1–39.

41. Serpell, L. C., Blake, C. C. F. and Fraser, P. E., Molecular structure of a fibrillar Alzheimer's Aβ fragment. *Biochemistry*, 2000, **39**, 13269–13275.

42. Tycko, R., Molecular structure of amyloid fibrils: insights from solid-state NMR. *Q. Rev. Biophys.*, 2006, **39**, 1–55.

43. Petkova, A. T., Ishii, Y., Balbach, J. J., Antzutkin, O. N., Leapman, R. D., Delaglio, F. and Tycko, R., A structural model for Alzheimer's β-amyloid fibrils based on experimental constraints from solid state NMR. *Proc. Natl. Acad. Sci. USA*, 2002, **99**, 16742–16747.

44. Petkova, A. T., Yau, W. and Tycko, R., Experimental constraints on quaternary structure in alzheimer's β-amyloid fibrils. *Biochemistry*, 2006, **45**, 498–512.

45. Tycko, R., Progress towards a molecular-level structural understanding of amyloid fibrils. *Curr. Opin. Struct. Biol.*, 2004, **14**, 96–103.

46. Antzutkin, O. N., Leapman, R. D., Balbach, J. J. and Tycko, R., Supramolecular structural constraints on Alzheimer's beta-amyloid fibrils from electron microscopy and solid-state nuclear magnetic resonance. *Biochemistry*, 2002, **41**, 15436–15450.

47. Nelson, R., Sawaya, M. R., Balbirnie, M., Madsen, A. Ø., Riekel, C., Grothe, R. and Eisenberg, D., Structure of the cross-β spine of amyloid-like fibrils. *Nature*, 2005, **435**, 773–778.

48. Sawaya, M. R. *et al.*, Atomic structures of amyloid cross-β spines reveal varied steric zippers. *Nature*, 2007, **447**, 453–457.

49. Ritter, C. *et al.*, Correlation of structural elements and infectivity of the HET-s prion. *Nature*, 2005, **435**, 844–848.

50. Perutz, M. F., Finch, J. T., Berriman, J. and Lesk, A., Amyloid fibers are water-filled nanotubes. *Proc. Natl. Acad. Sci. USA*, 2002, **99**, 5591–5595.

51. Singer, S. J. and Dewji, N. N., Evidence that Perutz's double-β-stranded subunit structure for β-amyloids also applies to their channel-forming structures in membranes. *Proc. Natl. Acad. Sci. USA*, 2006, **103**, 1546–1550.

52. Mukhopadhyay, S., Nayak, P. K., Udgaonkar, J. B. and Krishnamoorthy, G., Characterization of the formation of amyloid protofibrils from barstar by mapping residue-specific fluorescence dynamics. *J. Mol. Biol.*, 2006, **358**, 935–942.

53. Apetri, M. M., Maiti, N. C., Zagorski, M. G., Carey, P. R. and Anderson, V. E., Secondary structure of α-synuclein oligomers: characterization by raman and atomic force microscopy. *J. Mol. Biol.*, 2006, **355**, 63–71.

54. Kheterpal, I., Chen, M., Cook, K. D. and Wetzel, R., Structural differences in Aβ amyloid protofibrils and fibrils mapped by hydrogen exchange – mass spectrometry with on-line proteolytic fragmentation. *J. Mol. Biol.*, 2006, **361**, 785–795.

55. Walsh, D. M. *et al.*, Amyloid β-protein fibrillogenesis: structure and biological activity of protofibrillar intermediates. *J. Biol. Chem.*, 1999, **274**, 25945–25952.

56. Oosawa, F. and Kasai, M., A theory of linear and helical aggregations of macromolecules. *J. Mol. Biol.*, 1962, **4**, 10–21.

57. Goldstein, R. F. and Stryer, L., Cooperative polymerization reactions: analytical approximations, numerical examples, and experimental strategy. *Biophys. J.*, 1986, **50**, 583–599.

58. Flyvbjerg, H., Jobs, E. and Leibler, S., Kinetics of self-assembling microtubules: an 'inverse problem' in biochemistry. *Proc. Natl. Acad. Sci. USA*, 1996, **93**, 5975–5979.

59. Romberg, L., Simon, M. and Erickson, H. P., Polymerization of Ftsz, a bacterial homolog of tubulin. Is assembly cooperative? *J. Biol. Chem.*, 2001, **276**, 11743–11753.

60. Bishop, M. F. and Ferrone, F. A., Kinetics of nucleation-controlled polymerization. A perturbation treatment for use with a secondary pathway. *Biophys. J.*, 1984, **46**, 631–644.

61. Ferrone, F., Analysis of protein aggregation kinetics. *Meth. Enzymol.*, 1999, **309**, 256–274.

62. Harper, J. D. and Lansbury Jr, P. T., Models of amyloid seeding in Alzheimer's disease and scrapie: mechanistic truths and physiological consequences of the time-dependent solubility of amyloid proteins. *Annu. Rev. Biochem.*, 1997, **66**, 385–407.

63. Kodaka, M., Interpretation of concentration-dependence in aggregation kinetics. *Biophys. Chem.*, 2004, **109**, 325–332.

64. Wegner, A., Spontaneous fragmentation of actin filaments in physiological conditions. *Nature*, 1982, **296**, 266–267.

65. Wegner, A. and Savko, P., Fragmentation of actin filaments. *Biochemistry*, 1982, **21**, 1909–1913.

66. Ferrone, F. A., Sunshine, H. R., Hofrichter, J. and Eaton, W. A., Kinetic studies on photolysis-induced gelation of sickle cell hemoglobin suggest a new mechanism. *Biophys. J.*, 1980, **32**, 361–380.

67. Frieden, C., Protein aggregation processes: in search of the mechanism. *Protein Sci.*, 2007, **16**, 2334–2344.

68. Powers, E. T. and Powers, D. L., The kinetics of nucleated polymerizations at high concentrations: amyloid fibril formation near and above the 'supercritical concentration'. *Biophys. J.*, 2006, **91**, 122–132.

69. Booth, D. R. *et al.*, Instability, unfolding and aggregation of human lysozyme variants underlying amyloid fibrillogenesis. *Nature*, 1997, **385**, 787–793.

70. Kelly, J. W., The alternative conformations of amyloidogenic proteins and their multi-step assembly pathways. *Curr. Opin. Struct. Biol.*, 1998, **8**, 101–106.

71. Uversky, V. N. and Fink, A. L., Conformational constraints for amyloid fibril formation: the importance of being unfolded. *Biochim. Biophys. Acta*, 2004, **1698**, 131–153.

72. Colon, W. and Kelly, J. W., Partial denaturation of transthyretin is sufficient for amyloid fibril formation *in vitro*. *Biochemistry*, 1992, **31**, 8654–8660.

73. McCutchen, S. L., Colon, W., and Kelly, J. W., Transthyretin mutation Leu-55-Pro significantly alters tetramer stability and increases amyloidogenicity. *Biochemistry*, 1993, **32**, 12119–12127.

74. Lai, Z., Colon, W. and Kelly, J. W., The acid-mediated denaturation pathway of transthyretin yields a conformational intermediate that can self-assemble into amyloid. *Biochemistry*, 1996, **35**, 6470–6482.

75. Liu, K., Cho, H. S., Lashuel, H. A., Kelly, J. W. and Wemmer, D. E., A glimpse of a possible amyloidogenic intermediate of transthyretin. *Nat. Struct. Biol.*, 2000, **7**, 754–757.

76. McParland, V. J., Kalverda, A. P., Homans, S. W. and Radford, S. E., Structural properties of an amyloid precursor of β_2-microglobulin. *Nat. Struct. Biol.*, 2002, **9**, 326–331.

77. Hurle, M. R., Helms, L. R., Li, L., Chan, W. and Wetzel, R., A role for destabilizing amino acid replacements in light-chain amyloidosis. *Proc. Natl. Acad. Sci. USA*, 1994, **91**, 5446–5450.

78. Guijarro, J. I., Sunde, M., Jones, J. A., Campbell, I. D. and Dobson, C. M., Amyloid fibril formation by an SH3 domain. *Proc. Natl. Acad. Sci. USA*, 1998, **95**, 4224–4228.

79. Chiti, F., Taddei, N., Bucciantini, M., White, P., Ramponi, G. and Dobson, C. M., Mutational analysis of the propensity for amyloid formation by a globular protein. *EMBO J.*, 2000, **19**, 1441–1449.

80. Ramirez-Alvarado, M., Merkel, J. S. and Regan, L., A systematic exploration of the influence of the protein stability on amyloid fibril formation *in vitro*. *Proc. Natl. Acad. Sci. USA*, 2000, **97**, 8979–8984.

81. Jiang, X., Smith, C. S., Petrassi, H. M., Hammarstrom, P., White, J. T., Sacchettini, J. C. and Kelly, J. W., An engineered transthyretin monomer that is nonamyloidogenic, unless it is partially denatured. *Biochemistry*, 2001, **40**, 11442–11452.

82. Khurana, R., Gillespie, J. R., Talapatra, A., Minert, L. J., Ionescu-Zanetti, C., Millett, I. and Fink, A. L., Partially folded intermediates as critical precursors of light chain amyloid fibrils and amorphous aggregates. *Biochemistry*, 2001, **40**, 3525–3535.

83. Ahmad, A., Millett, I. S., Doniach, S., Uversky, V. N. and Fink, A. L., Partially folded intermediates in insulin fibril formation. *Biochemistry*, 2003, **42**, 11404–11416.

84. Chiti, F., Taddei, N., Stefani, M., Dobson, C. M. and Ramponi, G., Reduction of the amyloidogenicity of a protein by specific binding of ligands to the native conformation. *Protein Sci.*, 2001, **10**, 879–886.

85. Hamada, D. and Dobson, C. M., A kinetic study of β-lactoglobulin amyloid fibril formation promoted by urea. *Protein Sci.*, 2002, **11**, 2417–2426.

86. Chiti, F. and Dobson, C. M., Amyloid formation by globular proteins under native conditions. *Nat. Chem. Biol.*, 2009, **5**, 15–22.

87. Uversky, V. N., Li, J. and Fink, A. L., Trimethylamine-*N*-oxide-induced folding of alpha-synuclein. *FEBS Lett.*, 2001, **509**, 31–35.

88. Uversky, V. N. and Fink, A. L., Pathways to amyloid fibril formation: partially folded intermediates in the fibril formation of natively unfolded proteins. In *Amyloid Proteins, The Beta Sheet*

Conformation and Disease, Wiley-VCH Verlag GmbH & Co. KGaA, Weinheim, Germany, 2005, pp. 247–274.

89. Uversky, V. N., Li, J. and Fink, A. L., Evidence for a partially folded intermediate in alpha-synuclein fibril formation. *J. Biol. Chem.*, 2001, **276**, 10737–10744.

90. Wood, S. J., Wypych, J., Steavenson, S., Louis, J. C., Citron, M. and Biere, A. L., α-synuclein fibrillogenesis is nucleation-dependent. Implications for the pathogenesis of Parkinson's disease. *J. Biol. Chem.*, 1999, **274**, 19509–19512.

91. Baskakov, I. V. *et al.*, Self-assembly of recombinant prion protein of 106 residues. *Biochemistry*, 2000, **39**, 2792–2804.

92. Kundu, B., Maiti, N. R., Jones, E. M., Surewicz, K. A., Vanik, D. L. and Surewicz, W. K., Nucleation-dependent conformational conversion of the Y145Stop variant of human prion protein: Structural clues for prion propagation. *Proc. Natl. Acad. Sci. USA*, 2003, **100**, 12069–12074.

93. Collins, S. R., Douglass, A., Vale, R. D. and Weissman, J. S., Mechanism of prion propagation: amyloid growth occurs by monomer addition. *PLoS Biol.*, 2004, **2**, e321.

94. Gosal, W. S., Morten, I. J., Hewitt, E. W., Smith, D. A., Thomson, N. H. and Radford, S. E., Competing pathways determine fibril morphology in the self-assembly of β₂-microglobulin into amyloid. *J. Mol. Biol.*, 2005, **351**, 850–864.

95. Smith, A. M., Jahn, T. R., Ashcroft, A. E. and Radford, S. E., Direct observation of oligomeric species formed in the early stages of amyloid fibril formation using electrospray ionisation mass spectrometry. *J. Mol. Biol.*, 2006, **364**, 9–19.

96. Wang, X., Hammer, N. D. and Chapman, M. R., The molecular basis of functional bacterial amyloid polymerization and nucleation. *J. Biol. Chem.*, 2008, **283**, 21530–21539.

97. Baskakov, I. V. and Bocharova, O. V., *In vitro* conversion of mammalian prion protein into amyloid fibrils displays unusual features. *Biochemistry*, 2005, **44**, 2339–2348.

98. Xue, W. F., Homans, S. W. and Radford, S. E., Systematic analysis of nucleation-dependent polymerization reveals new insights into the mechanism of amyloid self-assembly. *Proc. Natl. Acad. Sci. USA*, 2008, **105**, 8926–8931.

99. Chen, S., Ferrone, F. A. and Wetzel, R., Huntington's disease age-of-onset linked to polyglutamine aggregation nucleation. *Proc. Natl. Acad. Sci. USA*, 2002, **99**, 11884–11889.

100. Bhattacharyya, A. M., Thakur, A. K. and Wetzel, R., Polyglutamine aggregation nucleation: thermodynamics of a highly unfavorable protein folding reaction. *Proc. Natl. Acad. Sci. USA*, 2005, **102**, 15400–15405.

101. Padrick, S. B. and Miranker, A. D., Islet amyloid: phase partitioning and secondary nucleation are central to the mechanism of fibrillogenesis. *Biochemistry*, 2002, **41**, 4694–4703.

102. Librizzi, F. and Rischel, C., The kinetic behavior of insulin fibril formation is determined by heterogeneous nucleation pathways. *Protein Sci.*, 2005, **14**, 3129–3134.

103. Ruschak, A. M. and Miranker, A. D., Fiber-dependent amyloid formation as catalysis of an existing reaction pathway. *Proc. Natl. Acad. Sci. USA*, 2007, **104**, 12341–12346.

104. Lomakin, A., Chung, D. S., Benedek, G. B., Kirschner, D. A. and Teplow, D. B., On the nucleation and growth of amyloid beta-protein fibrils: detection of nuclei and quantitation of rate constants. *Proc. Natl. Acad. Sci. USA*, 1996, **93**, 1125–1129.

105. Lomakin, A., Teplow, D. B., Kirschner, D. A. and Benedek, G. B., Kinetic theory of fibrillogenesis of amyloid beta-protein. *Proc. Natl. Acad. Sci. USA*, 1997, **94**, 7942–7947.

106. Goldsbury, C. S., Wirtz, S., Müller, S. A., Sunderji, S., Wicki, P., Aebi, U. and Frey, P., Studies on the *in vitro* assembly of Aβ 1–40: implications for the search for Aβ fibril formation inhibitors. *J. Struct. Biol.*, 2000, **130**, 217–231.

107. Serio, T. R. *et al.*, Nucleated conformational conversion and the replication of conformational information by a prion determinant. *Science*, 2000, **289**, 1317–1321.

108. Xu, S., Bevis, B. and Arnsdorf, M. F., The assembly of amyloidogenic yeast sup35 as assessed by scanning (atomic) force microscopy: an analogy to linear colloidal aggregation? *Biophys. J.*, 2001, **81**, 446–454.

109. Bitan, G., Kirkitadze, M. D., Lomakin, A., Vollers, S. S., Benedek, G. B. and Teplow, D. B., Amyloid β-protein (Aβ) assembly: Aβ 40 and Aβ 42 oligomerize through distinct pathways. *Proc. Natl. Acad. Sci. USA*, 2003, **100**, 330–335.

110. Gast, K. *et al.*, Effect of environmental conditions on aggregation and fibril formation of barstar. *Eur. Biophys. J.*, 2003, **32**, 710–723.

111. Carrotta, R., Manno, M., Bulone, D., Martorana, V. and San Biagio, P. L., Protofibril formation of amyloid β-protein at low pH via a non-cooperative elongation mechanism. *J. Biol. Chem.*, 2005, **280**, 30001–30008.

112. Goldsbury, C., Frey, P., Olivieri, V., Aebi, U. and Müller, S. A., Multiple assembly pathways underlie amyloid-β fibril polymorphisms. *J. Mol. Biol.*, 2005, **352,** 282–298.

113. Chimon, S., Shaibat, M. A., Jones, C. R., Calero, D. C., Aizezi, B. and Ishii, Y., Evidence of fibril-like β-sheet structures in a neurotoxic amyloid intermediate of Alzheimer's β-amyloid. *Nat. Struct. Mol. Biol.*, 2007, **14**, 1157–1164.

114. Kumar, S., Mohanty, S. K. and Udgaonkar, J. B., Mechanism of formation of amyloid protofibrils of barstar from soluble oligomers: evidence for multiple steps and lateral association coupled to conformational conversion. *J. Mol. Biol.*, 2007, **367**, 1186–1204.

115. Jain, S. and Udgaonkar, J. B., Evidence for stepwise formation of amyloid fibrils by the mouse prion protein. *J. Mol. Biol.*, 2008, **382**, 1228–1241.

116. Modler, A. J., Gast, K., Lutsch, G. and Damaschun, G., Assembly of amyloid protofibrils via critical oligomers – a novel pathway of amyloid formation. *J. Mol. Biol.*, 2003, **325**, 135–148.

117. Hurshman, A. R., White, J. T., Powers, E. T. and Kelly, J. W., Transthyretin aggregation under partially denaturing conditions is a downhill polymerization. *Biochemistry*, 2004, **43**, 7365–7381.

118. Baskakov, I. V., Legname, G., Baldwin, M. A., Prusiner, S. B. and Cohen, F. E., Pathway complexity of prion protein assembly into amyloid. *J. Biol. Chem.*, 2002, **277**, 21140–21148.

119. Walsh, D. M., Lomakin, A., Benedek, G. B., Condron, M. M. and Teplow, D. B., Amyloid β-protein fibrillogenesis: detection of a protofibrillar intermediate. *J. Biol. Chem.*, 1997, **272**, 22364–22372.

120. Nichols, M. R., Moss, M. A., Reed, D. K., Lin, W., Mukhopadhyay, R., Hoh, J. H. and Rosenberry, T. L., Growth of β-amyloid (1–40) protofibrils by monomer elongation and lateral association. Characterization of distinct products by light scattering and atomic force microscopy. *Biochemistry*, 2002, **41**, 6115–6127.

121. Ellisdon, A. M., Thomas, B. and Bottomley, S. P., The two-stage pathway of ataxin-3 fibrillogenesis involves a polyglutamine-independent step. *J. Biol. Chem.*, 2006, **281**, 16888–16896.

122. Esler, W. P. *et al.*, Alzheimer's disease amyloid propagation by a template-dependent dock-lock mechanism. *Biochemistry*, 2000, **39**, 6288–6295.

123. Scheibel, T., Bloom, J. and Lindquist, S. L., The elongation of yeast prion fibers involves separable steps of association and conversion. *Proc. Natl. Acad. Sci. USA*, 2004, **101**, 2287–2292.

124. Bessen, R. A. and Marsh, R. F., Biochemical and physical properties of the prion protein from two strains of the transmissible mink encephalopathy agent. *J. Virol.*, 1992, **66**, 2096–2101.

125. DePace, A. H. and Weissman, J. S., Origins and kinetic consequences of diversity in Sup35 yeast prion fibers. *Nat. Struct. Mol. Biol.*, 2002, **9**, 389–396.

126. Chien, P., DePace, A. H., Collins, S. R. and Weissman, J. S., Generation of prion transmission barriers by mutational control of amyloid conformations. *Nature*, 2003, **424**, 948–951.

127. Tanaka, M., Chien, P., Naber, N., Cooke, R. and Weissman, J. S., Conformational variations in an infectious protein determine prion strain differences. *Nature*, 2004, **428**, 323–328.

128. Makarava, N. and Baskakov, I. V., The same primary structure of the prion protein yields two distinct self-propagating states. *J. Biol. Chem.*, 2008, **283**, 15988–15996.

129. Hess, S., Lindquist, S. L. and Scheibel, T., Alternative assembly pathways of the amyloidogenic yeast prion determinant Sup35-NM. *EMBO Rep.*, 2007, **8**, 1196–1201.

130. Kad, N. M., Thomson, N. H., Smith, D. P., Smith, D. A. and Radford, S. E., β_2-microglobulin and its deamidated variant, N17D form amyloid fibrils with a range of morphologies *in vitro*. *J. Mol. Biol.*, 2001, **313**, 559–571.

131. Petkova, A. T., Leapman, R. D., Guo, Z., Yau, W., Mattson, M. P. and Tycko, R., Self-propagating, molecular-level polymorphism in Alzheimer's β-amyloid fibrils. *Science*, 2005, **307**, 262–265.

132. Kad, N. M., Myers, S. L., Smith, D. P., Smith, D. A., Radford, S. E. and Thomson, N. H., Hierarchical assembly of β_2-microglobulin amyloid *in vitro* revealed by atomic force microscopy. *J. Mol. Biol.*, 2003, **330**, 785–797.

133. Heise, H., Hoyer, W., Becker, S., Andronesi, O. C., Riedel, D. and Baldus, M., Molecular-level secondary structure, polymorphism, and dynamics of full-length α-synuclein fibrils studied by solid-state NMR. *Proc. Natl. Acad. Sci. USA*, 2005, **102**, 15871–15876.

134. Stine Jr, W. B. *et al.*, The nanometer-scale structure of amyloid-β visualized by atomic force microscopy. *J. Protein Chem.*, 1996, **15**, 193–203.

135. Bauer, H. H., Aebi, U., Häner, M., Hermann, R., Müller, M., Arvinte, T. and Merkle, H. P., Architecture and polymorphism of fibrillar supramolecular assemblies produced by *in vitro* aggregation of human calcitonin. *J. Struct. Biol.*, 1995, **115**, 1–15.

136. Goldsbury, C. S. *et al.*, Polymorphic fibrillar assembly of human amylin. *J. Struct. Biol.*, 1997, **119**, 17–27.

137. Cardoso, I. *et al.*, Transthyretin fibrillogenesis entails the assembly of monomers: a molecular model for *in vitro* assembled transthyretin amyloid-like fibrils. *J. Mol. Biol.*, 2002, **317**, 683–695.

138. Anderson, M., Bocharova, O. V., Makarava, N., Breydo, L., Salnikov, V. V. and Baskakov, I. V., Polymorphism and ultrastructural organization of prion protein amyloid fibrils: an insight from high resolution atomic force microscopy. *J. Mol. Biol.*, 2006, **358**, 580–596.

139. Benzinger, T. L., Gregory, D. M., Burkoth, T. S., Miller-Auer, H., Lynn, D. G., Botto, R. E. and Meredith, S. C., Propagating structure of Alzheimer's β-amyloid (10–35) is parallel β-sheet with residues in exact register. *Proc. Natl. Acad. Sci. USA*, 1998, **95**, 13407–13412.

140. Balbach, J. J. *et al.*, Amyloid fibril formation by $A\beta_{16-22}$, a seven-residue fragment of the Alzheimer's β-amyloid peptide, and structural characterization by solid state NMR. *Biochemistry*, 2000, **39**, 13748–13759.

141. Balbach, J. J., Petkova, A. T., Oyler, N. A., Antzutkin, O. N., Gordon, D. J., Meredith, S. C. and Tycko, R., Supramolecular structure in full-length Alzheimer's β-amyloid fibrils: evidence for a parallel β-sheet organization from solid-state nuclear magnetic resonance. *Biophys. J.*, 2002, **83**, 1205–1216.

142. Tycko, R. and Ishii, Y., Constraints on supramolecular structure in amyloid fibrils from two-dimensional solid-state NMR spectroscopy with uniform isotopic labeling. *J. Am. Chem. Soc.*, 2003, **125**, 6606–6607.

143. Petkova, A. T., Buntkowsky, G., Dyda, F., Leapman, R. D., Yau, W. M. and Tycko, R., Solid state NMR reveals a pH-dependent antiparallel β-sheet registry in fibrils formed by a β-amyloid peptide. *J. Mol. Biol.*, 2004, **335**, 247–260.

144. Jimenez, J. L., Nettleton, E. J., Bouchard, M., Robinson, C. V., Dobson, C. M. and Saibil, H. R., The protofilament structure of insulin amyloid fibrils. *Proc. Natl. Acad. Sci. USA*, 2002, **99**, 9196–9201.

145. Calamai, M., Chiti, F. and Dobson, C. M., Amyloid fibril formation can proceed from different conformations of a partially unfolded protein. *Biophys. J.*, 2005, **89**, 4201–4210.

146. Song, J., Jamin, N., Gilquin, B., Vita, C. and Menez, A., A gradual disruption of tight side-chain packing: 2D 1H-NMR characterization of acid-induced unfolding of CHABII. *Nat. Struct. Biol.*, 1999, **6**, 129–134.

147. Lakshmikanth, G. S., Sridevi, K., Krishnamoorthy, G. and Udgaonkar, J. B., Structure is lost incrementally during the unfolding of barstar. *Nat. Struct. Mol. Biol.*, 2001, **8**, 799–804.

148. Kuzmenkina, E. V., Heyes, C. D. and Nienhaus, G. U., Single-molecule FRET study of denaturant induced unfolding of RNase H. *J. Mol. Biol.*, 2006, **357**, 313–324.

149. Sadqi, M., Fushman, D. and Munoz, V., Atom-by-atom analysis of global downhill protein folding. *Nature*, 2006, **442**, 317–321.

150. Crick, S. L., Jayaraman, M., Frieden, C., Wetzel, R. and Pappu, R. V., Fluorescence correlation spectroscopy shows that monomeric polyglutamine molecules form collapsed structures in aqueous solutions. *Proc. Natl. Acad. Sci. USA*, 2006, **103**, 16764–16769.

151. Zhang, S. *et al.*, The Alzheimer's peptide Aβ adopts a collapsed coil structure in water. *J. Struct. Biol.*, 2000, **130**, 130–141.

152. Lee, J. C., Lai, B. T., Kozak, J. J., Gray, H. B. and Winkler, J. R., α-synuclein tertiary contact dynamics. *J. Phys. Chem. B*, 2007, **111**, 2107–2112.

153. Mukhopadhyay, S., Krishnan, R., Lemke, E. A., Lindquist, S. and Deniz, A. A., A natively unfolded yeast prion monomer adopts an ensemble of collapsed and rapidly fluctuating structures. *Proc. Natl. Acad. Sci. USA*, 2007, **104**, 2649–2654.

154. Lashuel, H. A., Petre, B. M., Wall, J., Simon, M., Nowak, R. J., Walz, T. and Lansbury, P. T., α-Synuclein, especially the Parkinson's disease-associated mutants, forms pore-like annular and tubular protofibrils. *J. Mol. Biol.*, 2002, **322**, 1089–1102.

155. Lashuel, H. A. *et al.*, Hartley, D., Petre, B. M., Walz, T. and Lansbury Jr, P. T., Amyloid pores from pathogenic mutations. *Nature*, 2002, **418**, 291.

156. Relini, A. *et al.*, Monitoring the process of HypF fibrillization and liposome permeabilization by protofibrils. *J. Mol. Biol.*, 2004, **338**, 943–957.

157. Kayed, R. *et al.*, Annular protofibrils are a structurally and functionally distinct type of amyloid oligomer. *J. Biol. Chem.*, 2009, **284**, 4230–4237.

158. Caughey, B. and Lansbury, P. T., Protofibrils, pores, fibrils, and neurodegeneration: separating the responsible protein aggregates from the innocent bystanders. *Annu. Rev. Neurosci.*, 2003, **26**, 267–298.

159. Kayed, R., Sokolov, Y., Edmonds, B., McIntire, T. M., Milton, S. C., Hall, J. E. and Glabe, C. G., Permeabilization of lipid bilayers is a common conformation-dependent activity of soluble amyloid oligomers in protein misfolding disease. *J. Biol. Chem.*, 2004, **279**, 46363–46366.

160. Quist, A. *et al.*, Amyloid ion channels: a common structural link for protein-misfolding disease. *Proc. Natl. Acad. Sci. USA*, 2005, **102**, 10427–10432.

161. Lashuel, H. A., Lai, Z., and Kelly, J. W., Characterization of the transthyretin acid denaturation pathways by analytical ultracentrifugation: implications for wild-type, V30M, and L55P amyloid fibril formation. *Biochemistry*, 1998, **37**, 17851–17864.

162. Huang, T. H. J., Yang, D. S., Plaskos, N. P., Go, S., Yip, C. M., Fraser, P. E. and Chakrabartty, A., Structural studies of soluble oligomers of the Alzheimer β-amyloid peptide. *J. Mol. Biol.*, 2000, **297**, 73–87.

163. Mastrangelo, I. A., Ahmed, M., Sato, T., Liu, W., Wang, C., Hough, P. and Smith, S. O., High-resolution atomic force microscopy of soluble Aβ42 oligomers. *J. Mol. Biol.*, 2006, **358**, 106–119.

164. Ding, T. T., Lee, S., Rochet, J. and Lansbury Jr, P. T., Annular α-synuclein protofibrils are produced when spherical protofibrils are incubated in solution or bound to brain-derived membranes. *Biochemistry*, 2002, **41**, 10209–10217.

165. Seshadri, S., Khurana, R. and Fink, A. L., Fourier transform infrared spectroscopy in analysis of protein deposits. *Methods Enzymol.*, 1999, **309**, 559–576.

166. Zandomeneghi, G., Krebs, M. R. H., Mccammon, M. G. and Fändrich, M., FTIR reveals structural differences between native β-sheet proteins and amyloid fibrils. *Protein Sci.*, 2004, **13**, 3314–3321.

167. Susi, H., Infrared spectroscopy – conformation. *Methods Enzymol.*, 1972, **26**, 455–472.

168. Chiti, F., Stefani, M., Taddei, N., Ramponi, G. and Dobson, C. M., Rationalization of the effects of mutations on peptide and protein aggregation rates. *Nature*, 2003, **424**, 805–808.

169. DuBay, K. F., Pawar, A. P., Chiti, F., Zurdo, J., Dobson, C. M. and Vendruscolo, M., Prediction of the absolute aggregation rates of amyloidogenic polypeptide chains. *J. Mol. Biol.*, 2004, **341**, 1317–1326.

170. Thakur, A. K. *et al.*, Polyglutamine disruption of the huntingtin exon 1 N terminus triggers a complex aggregation mechanism. *Nat. Struct. Mol. Biol.*, 2009, **16**, 380–389.

171. Smith, D. P., Jones, S., Serpell, L. C., Sunde, M. and Radford, S. E., A systematic investigation into the effect of protein destabilisation on β_2-microglobulin amyloid formation. *J. Mol. Biol.*, 2003, **330**, 943–954.

172. Platt, G. W., Routledge, K. E., Homans, S. W. and Radford, S. E., Fibril growth kinetics reveal a region of β2-microglobulin important for nucleation and elongation of aggregation. *J. Mol. Biol.*, 2008, **378**, 251–263.

173. Bocharova, O. V., Breydo, L., Parfenov, A. S., Salnikov, V. V. and Baskakov, I. V., *In vitro* conversion of full-length mammalian prion protein produces amyloid form with physical properties of PrP^{Sc}. *J. Mol. Biol.*, 2005, **346**, 645–659.

174. Baskakov, I. V., Legname, G., Prusiner, S. B. and Cohen, F. E., Folding of prion protein to its native α-helical conformation is under kinetic control. *J. Biol. Chem.*, 2001, **276**, 19687–19690.

175. Khurana, R. and Udgaonkar, J. B., Equilibrium unfolding studies of barstar: evidence for an alternative conformation which resembles a molten globule. *Biochemistry,* 1994, **33**, 106–115.

176. Swaminathan, R., Periasamy, N., Udgaonkar, J. B. and Krishnamoorthy, G., Molten globule-like conformation of barstar: a study by fluorescence dynamics. *J. Phys. Chem.*, 1994, **98**, 9270–9278.

177. Juneja, J., Bhavesh, N. S., Udgaonkar, J. B. and Hosur, R. V., NMR identification and characterization of the flexible regions in the 160 kD molten globule-like aggregate of barstar at low pH. *Biochemistry*, 2002, **41**, 9885–9899.

178. Lomakin, A., Benedek, G. B. and Teplow, D. B., Monitoring protein assembly using quasielastic light scattering microscopy. *Methods Enzymol.*, 1999, **309**, 429–459.

179. Kowalewski, T. and Holtzman, D. M., *In situ* atomic force microscopy study of Alzheimer's β-amyloid peptide on different substrates: new insights into mechanism of β-sheet formation. *Proc. Natl. Acad. Sci. USA*, 1999, **96**, 3688–3693.

180. Nybo, M., Svehag, S. E. and Nielsen, E. H., An ultrastructural study of amyloid intermediates in Aβ1-42 fibrillogenesis. *Scand. J. Immunol.*, 1999, **49**, 219–223.

181. Blackley, H. K. L., Sanders, G. H. W., Davies, M. C., Roberts, C. J., Tendler, S. J. B. and Wilkinson, M. J., *In-situ* atomic force microscopy study of β-amyloid fibrillization. *J. Mol. Biol.*, 2000, **298**, 833–840.

182. Bitan, G., Lomakin, A. and Teplow, D. B., Amyloid β-protein oligomerization. *J. Biol. Chem.*, 2001, **276**, 35176–35184.

183. Slepko, N., Bhattacharyya, A. M., Jackson, G. R., Steffan, J. S., Marsh, J. L., Thompson, L. M., and Wetzel, R., Normal-repeat-length polyglutamine peptides accelerate aggregation nucleation and cytotoxicity of expanded polyglutamine proteins. *Proc. Natl. Acad. Sci. USA*, 2006, **103**, 14367–14372.

184. Bhattacharyya, A. *et al.*, Oligoproline effects on polyglutamine conformation and aggregation. *J. Mol. Biol.*, 2006, **355**, 524–535.